TRANSIENT STABILITY ANALYSIS OF A GRID CONNECTED DOUBLY FED INDUCTION GENERATOR

A DISSERTATION

Submitted in partial fulfillment of the requirements for the award of the degree
of
MASTER OF TECHNOLOGY
in
ELECTRICAL ENGINEERING
(With Specialization in Power System Engineering)

By

G13690 **SHERI SUNDEEP**

DEPARTMENT OF ELECTRICAL ENGINEERING
INDIAN INSTITUTE OF TECHNOLOGY ROORKEE
ROORKEE - 247 667 (INDIA)
JUNE, 2008

Dedicated to
My Loving Parents & Sisters

INDIAN INSTITUTE OF TECHNOLOGY
ROORKEE
ROORKEE

CANDIDATE'S DECLARATION

I hereby declare that the work that is being presented in this dissertation report entitled **"TRANSIENT STABILITY ANALYSIS OF A GRID CONNECTED DOUBLY FED INDUCTION GENERATOR"** submitted in partial fulfillment of the requirements for the award of the degree of **Master of Technology** with specialization in **Power System Engineering**, to the Department of Electrical Engineering, Indian Institute of Technology, Roorkee, is an authentic record of my own work carried out, under the esteemed guidance of, Dr. Biswarup Das & Dr. Vinay Pant, Department of Electrical Engineering, Indian Institute of Technology, Roorkee.

I have not submitted the matter presented in this dissertation report for the Award of any other degree or diploma.

Date: **(SHERI SUNDEEP)**

Place: Roorkee **En. No. : 064010**

This is to certify that the above statement made by the candidate is correct to the best of my knowledge.

Dr. BISWARUP DAS
Associate Professor

Dr. VINAY PANT
Assistant Professor

Department of Electrical Engineering
Indian Institute of Technology
ROORKEE - 247 667

ACKNOWLEDGEMENT

It is my proud privilege to express my deep sense of gratitude and indebtedness towards my guides Dr. Biswarup Das, Associate Professor and Dr. Vinay Pant, Assistant Professor, Department of Electrical Engineering, IIT Roorkee, for their invaluable guidance & criticism, which were vital in successful completion of the present work. Their moral & technical support, and enthusiasm has had always given me confidence and encouragement in doing my dissertation work with joy and interest. I am heartily thankful to them for their constant assistance and suggestions, without which it would have not been possible to compile this report in the present form.

I express my deep sense of gratitude to Dr. J. D. Sharma and Dr. N.P. Padhy, Professors, Department of Electrical Engineering, IIT Roorkee, for giving me an opportunity to work in the CAD-Lab.

I would like to thank Prof. M. K. Vasantha, for his constant happy time wishes, which filled me with joy and enthusiasm.

I wish to thank Mr. J. Upender, Mr. Deepak Nagaria, Mr. Arup Goswamy, Mr. Kawardeep Singh and Mr. Rohith Bhakar, PhD. scholars, Department of Electrical Engineering, IIT Roorkee, for their regular encouragement, and moral and technical support.

I like to thank my friend, Mr. V. S. Sriram, for being besides me at times of need.

I would like to thank all those who are involved directly or indirectly for completion of my dissertation work.

My sincere, heartfelt gratitude and indebtedness to my parents and sisters, whose efforts, prayers and blessings, have given courage and strength to my life.

(Sheri Sundeep)

ABSTRACT

In the wake of energy crisis, the world economy is determined to capture the untapped renewable energy potential. Wind energy, due to its free availability and clean character, ranks as the most promising renewable energy resource that can play a key role in solving the world energy crisis.

This dissertation deals with the modelling and transient stability analysis of Doubly Fed Induction Generator (DFIG) for wind turbines connected to grid system. A reduced order model for the DFIG has been used. A controller for speed, voltage and power factor has also been implemented. The DFIG model and the controller are presented as Differential Algebraic Equations (DAE). A 7^{th} order model for synchronous machine with IEEE type-I exciter has also been presented.

The DAEs have been solved using Simultaneous Implicit (SI) method. SI-method is a numerical method that is widely used in industries now-a-days. The derivations using the SI-method for TSA simulations have been presented in detail. Particle Swarm Optimization (PSO) has been implemented to optimize the DFIG controller gains.

TSA simulation results for three 8 bus power system networks, with DFIG and infinite bus, with only synchronous machine and with DFIG and synchronous machine in the network, have been presented.

LIST OF CONTENTS

LIST OF FIGURES

LIST OF TABLES

List of Symbols

Symbol	Symbol description
i_{ds} :	DFIG d-axis stator current
i_{qs} :	DFIG q-axis stator current
v_{ds} :	DFIG d-axis stator voltage
v_{qs} :	DFIG q-axis stator voltage
e_d :	DFIG d-axis voltage behind transient reactance
e_q :	DFIG q-axis voltage behind transient reactance
i_{dr} :	DFIG d-axis rotor current
i_{qr} :	DFIG q-axis rotor current
v_{dr} :	DFIG d-axis rotor voltage
v_{qr} :	DFIG q-axis rotor voltage
ω_r :	DFIG rotor angular speed
ω_s :	Synchronous speed
v_{ref} :	DFIG reference voltage
s :	Slip
T_m :	DFIG mechanical torque
H_t :	DFIG inertia constant
L_m :	DFIG mutual inductance
L_s :	DFIG stator inductance
L_r :	DFIG rotor inductance
K_p, K_I :	Controller proportional and integral gains
$P_{opt}, T_{opt}, K_{opt}$:	Optimal power, torque and turbine constant
X', X :	DFIG transient and open circuit reactance
R_s, R_r :	DFIG stator and rotor resistance
E_d' :	Synchronous machine d-axis voltage behind transient reactance
E_q' :	Synchronous machine q-axis voltage behind transient reactance
δ :	Synchronous machine internal angle
ω :	Synchronous machine angular speed
E_{fd} :	Synchronous machine exciter output voltage
V_R :	Synchronous machine regulator output
I_d :	Synchronous machine d-axis machine generated current
I_q :	Synchronous machine q-axis machine generated current

V : Terminal voltage

θ : Terminal angle

V_{ref} : Synchronous machine voltage reference

R_S : Synchronous machine stator resistance

X_d, X_q : Synchronous machine unsaturated d- and q-axis synchronous reactance

$X_d^{'}, X_q^{'}$: Synchronous machine unsaturated d- and q-axis transient reactance

$T_{do}^{'}, T_{qo}^{'}$: Synchronous machine transient open circuit d- and q-axis time constant

D : Synchronous machine load damping coeffient

Chapter 1
INTRODUCTION

The world is entering into a new phase. A phase of climate shifts. With increasing developments in the field of industrialisation and the usage of fossil fuels has made this earth an unsafe place to live. If this continues life on earth may end exponentially. But, the situation can be controlled if we can act immediately. This can be done by reducing the use of fossil fuels and encouraging the use of cleaner and greener fuels.

There are many sources of clean and green fuels/energy. For example, wind, solar, tidal, etc. Wind energy sector is one sector which is getting the highest attention.

1.1 Wind Energy: India

The Indian wind energy sector has an installed capacity of 8757.2 MW (as on March 31, 2008). In terms of wind power installed capacity, India is ranked 4th in the World [1]. Today India is a major player in the global wind energy market. Table 1.1 gives the performance and ranking of the top ten countries in the world [2].

The potential is far from exhausted. Indian Wind Energy Association has estimated that with the current level of technology, the 'on-shore' potential for utilization of wind energy for electricity generation is of the order of 65,000 MW. This enormous unexploited resource availability has the potential to sustain the growth of wind energy sector in India in the years to come [1].

With such a high potential, wind energy systems integration into the electrical power system grid can release some pressure on the generating stations running on fossil fuels and hence on earth.

1.2 Wind Turbine (WT) Generators

The WT generator converts mechanical energy to electrical energy. WT generators are a bit unusual, compared to other generating units attached to the electrical grid. One of the reasons is that the generator has to work with a power source (the WT rotor) which supplies very fluctuating mechanical power (torque).

Table 1.1: Performance and ranking of the top ten countries in the world in the wind energy sector.

Ranking total 2007	**Country**	**Total Capacity installed end 2007**	**Additional Capacity 2007 (Difference 2007-2006)**	**Rate of Growth 2007**	**Ranking total 2006**	**Total Capacity installed end 2006**	**Total Capacity installed end 2005**
		[MW]	[MW]	[%]		[MW]	[MW]
1	Germany	22,247.4	1625.4	7.9	1	20,622.0	18,427.5
2	USA	16,818.8	5215.8	45.0	3	11,603.0	9,149.0
3	Spain	15,145.1	3515.1	30.2	2	11,630.0	10,027.9
4	India	7,850.0	1580.0	25.2	4	6,270.0	4,430.0
5	China	5,899.0	3300.0	127.0	6	2,599.0	1,266.0
6	Denmark	3,125.0	-11.0	-0.4	5	3,136.0	3,128.0
7	Italy	2,726.1	602.7	28.4	7	2,123.4	1,718.3
8	France	2,455.0	888.0	56.7	10	1,567.0	757.2
9	United Kingdom	2,389.0	426.2	21.7	8	1,962.9	1,353.0
10	Portugal	2,130.0	414.0	24.1	9	1,716.0	1,022.0

Common voltage rating of the generator is 690V AC. This voltage is then transformed to higher voltages through transformers inorder to integrate it into the grid. Commonly used first step-up voltages are 11 kV and 33 kV. WT generators are available with both 50 Hz and 60 Hz frequency rating. The world's largest WT is now the Enercon E-126 installed in Emden, Germany by Enercon. This turbine is officially rated at 6 megawatts, but is capable of producing 7+ MW (or 20 million kilowatt hours per year) [3].

Wind turbines may be designed with either synchronous or asynchronous generators, and with various forms of direct or indirect grid connection of the generator. Direct grid connection mean that the generator is connected directly to the (usually 3-phase) alternating current grid. Indirect grid connection means that the current from the turbine passes through a series of electric devices which adjust the electrical parameters to match that of the grid.

Asynchronous generators are further categorized as singly-fed and doubly-fed generators.

1. **Singly-Fed Asynchronous Generators (SFAG):** SFAG belong to that category of electric machines which incorporate one multiphase winding set, which is independently excited, actively participates in the energy conversion

process (i.e., is singly-fed), and determines the full electro-mechanical conversion power rating of the machine. The principle purpose of the squirrel-cage rotor winding or wound rotor winding of the Induction machine is to develop a rotating magnetic field in the air-gap. The electrical power contribution of these windings is dissipative and accordingly, these windings do not actively participate in the energy conversion process (i.e., passive winding set) [4].

2. **Doubly-Fed Asynchronous generator (DFAG):** DFAG belongs to a category of electric machines that incorporate two multiphase winding sets of similar power rating that have independent means of excitation. As a result, doubly-fed electric machines are synchronous electric machines by nature but with both winding sets actively participating in the energy conversion process (i.e., doubly-fed or dual armature) [5].

   DFAGs can operate at constant torque to twice synchronous speed for a given frequency of excitation with each active winding set having similar power ratings (i.e., contiguous operation between sub-synchronous through super-synchronous speed range). The sum of the power ratings of the multiphase winding sets determine the total electro-mechanical conversion power rating of the machine.

A commonly used DFAG now-a-days is Doubly Fed Induction Generator or commonly know as DFIG. It is based on an induction generator with a multiphase wound rotor and a multiphase slipring assembly with brushes for access to the rotor (wound-rotor doubly-fed). But in recent machines efforts have been made to avoid the multiphase slipring assembly with brushes (brushless wound-rotor doubly-fed electric machines).

1.3 Literature Review

In early days, most national network design codes and standards did not require wind farms to support the power system during a disturbance. But with increasing penetration of wind farms and usage of DFIGs into the power system network and its operation, national network design codes and standards expect wind farms to support the power system during disturbances. But in order to study the

effect of wind farm/DFIG penetration into the power system network they have to be modeled suitably and represented. Several papers have been presented in this field of dynamic modelling of DFIG.

Dynamic model of a variable speed (VS) WT with DFIG and back to back voltage source converter (BVSC) and its controls has been presented in [6]. In this work, a 5th order dynamic model with synchronously rotating d-q axis reference frame and with q axis leading has been derived. Speed control, pitch control and voltage control are included in the model.

Phasors represented with respect to different rotating reference frames has been presented in [7]. The paper has proposed speed and pitch angle control model.

Janaka B. Ekanayake et. al. [8] has presented a model that can be used for single-cage and double-cage representation of the DFIG and its control and protection circuits. The paper has presented a 3rd order dynamic model with synchronously rotating reference frame and with q axis leading the d-axis. A controller which controls terminal voltage, speed and power factor has also been developed. Similar models were also presented in [9, 10, 11]. It is to be noted that the works presented in [7-10] have used time domain analysis approach.

In [12] a PSS for a DFIG based wind generation has been proposed. It uses Flux Magnitude Angle Control (FMAC) approach for control. Both eigenvalue and time domain approaches have been used for analysis.

A 7th order model has been presented in [13], which uses the modal analysis approach along with eigenvalue analysis. Pablo Ledesma et. al. [14] have used Simultaneous Implicit method of numerical simulation with the static model of the electric Grid for transient stability analysis.

1.4 Present Work

Different types of WT generators behave differently during transmission grid disturbances. In particular, induction generators cannot support the system voltage during faults, unlike steam or hydro turbine-driven synchronous generators. However, DFIG permits variable rotor speed operation, and provides independent control of active and reactive power flows into and out of the generator and hence desirable properties for grid interconnection. Therefore, extensive modeling of the dynamic electromechanical

characteristics of a new wind farm is required by transmission system operators to ensure predictable stable behaviour during system faults.

In this thesis, titled "Transient Stability Analysis of a Grid Connected Doubly-Fed Induction Generator", a DFIG has been modelled mathematically and simulated for transient stability analysis (TSA). The DFIG has been interconnected to a grid system and a fault has been simulated on one of the buses. The behaviour of DFIG with and without synchronous machine under the fault condition has been observed.

In the present work, an 8 bus power system network as in [9] has been considered for simulation purpose. Using this network, simulation studies have been carried out in three parts. First, a DFIG and a grid (in this case an Infinite bus) system has been used. Then the network has been modified by connecting a synchronous machine without the DFIG. Then synchronous machine and DFIG together have been connected and TSA studies have been carried out.

Following is the sequence in which the work has been carried out.

1. Power System Mathematical Modelling
2. Derivations for TSA using Simultaneous Implicit (SI) Method
3. Coding and Simulation

Chapter 1 has given a brief introduction on wind energy in India, WT generators and a brief description of the present work in this dissertation.

Chapter 2 gives various derivations and mathematical model for the power system network which includes modelling of the infinite bus, synchronous machines, DFIGs and the network.

Chapter 3 describes the derivations required for TSA using the SI method. This chapter also describes procedure for finding the initial conditions for the DFIG and the synchronous machine.

Chapter 4 gives the simulation results and analysis for the 8-bus DFIG-infinite bus system.

Chapter 5 gives simulation results for the 8-bus synchronous machine system and 8-bus DFIG-synchronous machine system.

And finally the last chapter gives the conclusion and future scope.

Chapter 2

POWER SYSTEM MODELLING

2.1 Introduction:

In this chapter, the various power system elements have been modelled mathematically. The various power system elements considered for modelling are: the Infinite Bus, Synchronous Machine, DFIG, Loads and the Network.

Consider a 'n' bus, 'm' machine power system, in which, without any loss of generality, it is assumed that the 'm' synchronous machines are connected at the first 'm' buses of the system. It is also assumed that there are 'g' DFIGs installed in the system which are connected at bus numbers 'm+1', 'm+2', ... 'm+g'.

2.2 Synchronous machine Modeling [15]

The synchronous machine model considered here is a 7th order model and an exciter of Type-I. The various assumptions considered are as in accordance with [15].

2.2.1 Differential Equations:

$$T'_{doi}\frac{dE'_{qi}}{dt} = -E'_{qi} - (X_{di} - X'_{di})I_{di} + E_{fdi} \tag{2.1}$$

$$T'_{qoi}\frac{dE'_{di}}{dt} = -E'_{di} - (X_{qi} - X'_{qi})I_{qi} \tag{2.2}$$

$$\frac{d\delta_i}{dt} = (\omega_i - \omega_s) \tag{2.3}$$

$$\frac{2H_i}{\omega_s}\frac{d\omega_i}{dt} = T_{Mi} - E'_{di}I_{di} - E'_{di}I_{di} - (X'_{qi} - X'_{di})I_{di}I_{qi} - D_i(\omega_i - \omega_s) \tag{2.4}$$

$$T_{Ei}\frac{dE_{fdi}}{dt} = -(K_{Ei} + S_{Ei}(E_{fdi}))E_{fdi} + V_{Ri} \tag{2.5}$$

$$T_{Fi}\frac{dR_{fi}}{dt} = -R_{fi} + \frac{K_{Fi}}{T_{Fi}}E_{fdi} \tag{2.6}$$

$$T_{Ai}\frac{dV_{Ri}}{dt} = -V_{Ri} + K_{Ai}R_{fi} - \frac{K_{Ai}K_{Fi}}{T_{Fi}}E_{fdi} + K_{Ai}(V_{refi} - V_i) \tag{2.7}$$

Where, $i = 1, 2, 3 \ldots m$

2.2.2 Stator Algebraic Equations

Fig. 2.1 [15] shows synchronous machine two axis dynamic model.

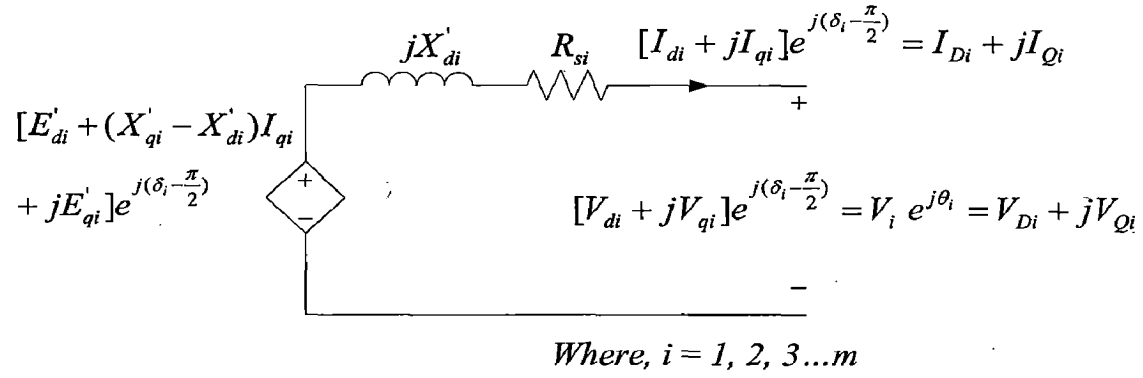

Figure 2.1: Synchronous machine two axis dynamic circuit

Applying Kirchhoff's Voltage Law (KVL) to the above model and multiplying both the sides by $e^{-j(\delta_i - \frac{\pi}{2})}$ and equating real and imaginary parts, we can write the stator equations in the *polar form* as:

$$E'_{di} - V_i \sin(\delta_i - \theta_i) - R_{Si} I_{di} + X'_{qi} I_{qi} = 0 \qquad (2.8)$$

$$E'_{qi} - V_i \cos(\delta_i - \theta_i) - R_{Si} I_{qi} - X'_{di} I_{di} = 0 \qquad (2.9)$$

Where, $i = 1, 2, 3 \ldots m$

2.3 DFIG Modeling

WTs and wind parks have to be considered in power system dynamic stability studies for which, however, suitable WT models are needed. These models have to compromise between accuracy, for considering relevant dynamic interactions between grid and WT, and simplicity required for the simulation of large systems.

As stated earlier, DFIG is based on an induction generator principle and incorporate two multiphase winding sets of similar power rating that have independent means of excitation. Fig. 2.2 shows representation of grid connected DFIG [10]. The DFIG transforms the input turbine power into electrical power. The produced stator power is always positive. The rotor power can be both positive and negative due to the presence of the back-to-back converter. DFIG connects to the grid with a back-to-back voltage source converter which controls the excitation system. This is in order to decouple the mechanical and electrical rotor frequency. The rotor side converter works at the rotor frequency while the grid side converter works at grid

frequency. The variable frequency rotor voltage permits the adjustment of the rotor speed to match the optimum operating point at any practical wind speed [7]. The rotor side converter is typically used by many manufacturers to control the speed together with terminal voltage and power factor. While the grid side converter, as a shunt reactive power converter, is also used to charge the DC link and maintain the link voltage.

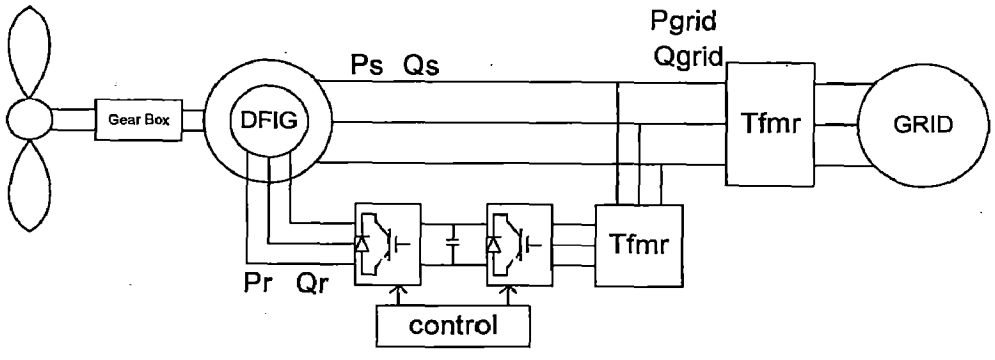

Figure 2.2: Representation of grid connected DFIG

Fig. 2.3 shows the equivalent vector representation of operating condition of a DFIG [12]. In this figure, e_g represents the internally generated voltage vector in the stator or commonly known as the voltage behind transient reactance. The magnitude of e_g depends on the magnitude of the rotor flux vector, ψ_r. This flux is dependent on the generator stator and rotor currents but can be controlled by adjustment of the rotor voltage vector, v_r. Synchronously rotating reference frame is chosen with the q-axis aligning with the stator terminal voltage vector v_s. The angle δ_g defines the position of e_g with respect to v_s. δ_g is determined by the power output of the generator.

DFIG is capable of generating basically in two modes. One is in sub-synchronous speed mode, wherein the rotor absorbs power and part of the generated power by the stator enters the rotor circuit. The other is the super-synchronous speed mode, wherein the rotor generates power and delivers to the grid. Hence the total power generator by the DFIG is the sum/difference of the powers generated/absorbed by the stator and the rotor respectively.

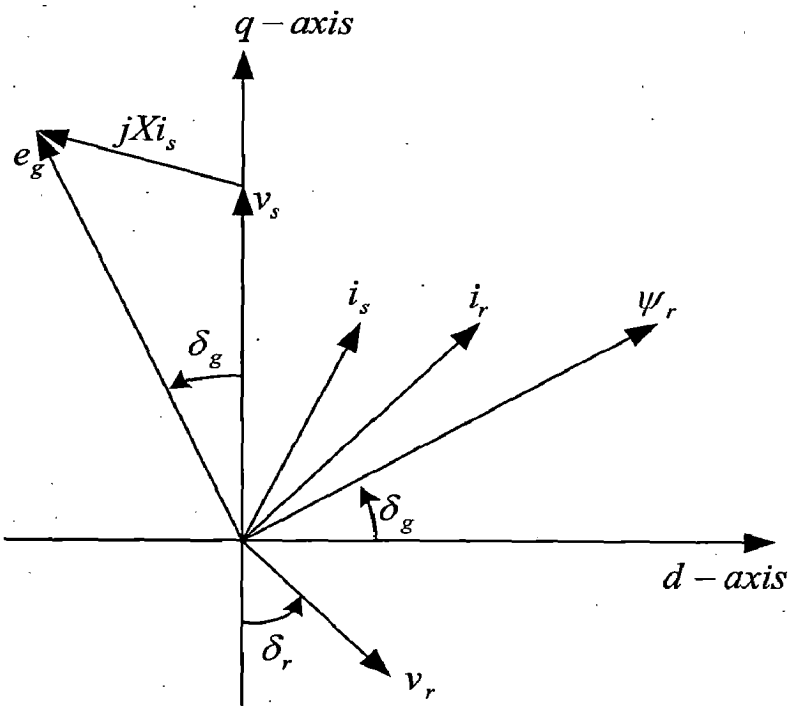

Figure 2.3: Vector Representation of operating conditions of a DFIG

For modeling the DFIG, a 5th order model, as described in [10], was reduced to 3rd order by neglecting the DC component in the stator transient current and thus allowing only fundamental frequency components. This facilitates a good compromise between simplicity and accuracy. Here, the converters have been considered ideal and the DC link voltage has been assumed to be constant [10]. Also, a controller as used in [9] for rotor voltages has been used in this work. The dynamics of the controller can be described by three more differential equations. Thus, it may be considered as a 6th order model as well.

In modelling the DFIG, the generator convention was adopted and the synchronously rotating d-q axis reference frame (ω_s) with q axis leading the d-axis has been considered. Stator d- and q- axis currents flowing towards the grid were considered as positive while rotor d- and q- axis currents were considered as negative.

2.3.1 Machine Differential-Algebraic equations [10]

$$-R_{si}i_{dsi} + X_i'i_{qsi} + e_{di} - V_i\cos\theta_i = 0 \tag{2.10}$$

$$-R_{si}i_{qsi} - X_i'i_{dsi} + e_{qi} - V_i\sin\theta_i = 0 \tag{2.11}$$

$$\frac{de_{di}}{dt} = -\frac{1}{T_{oi}}[e_{di} - (X_i - X_i')i_{qsi}] + s\omega_s e_{qi} - \omega_s \frac{L_{mi}}{L_{rri}} v_{qri} \tag{2.12}$$

$$\frac{de_{qi}}{dt} = -\frac{1}{T_{oi}}[e_{qi} + (X_i - X_i')i_{dsi}] - s\omega_s e_{di} + \omega_s \frac{L_{mi}}{L_{rri}} v_{dri} \tag{2.13}$$

Rotor Swing Equation [9, 10, 11]:

$$\frac{d\omega_{ri}}{dt} = \frac{1}{2H_{ti}}\left[T_{mi} + \frac{V_i i_{qsi}}{\omega_{si}}\right] \tag{2.14}$$

Where, $i = 1, 2, 3 \ldots g$

2.3.2 Controller Differential-Algebraic equations

Controller equations have been derived using the controller block given in [12] and shown here in Fig. 2.4. This controller is capable of controlling the rotor d-axis and q-axis voltages namely, v_{dr} and v_{qr} respectively. The rotor speed was considered to be controlled by v_{qr} and the terminal voltage and power factor by v_{dr} [10].

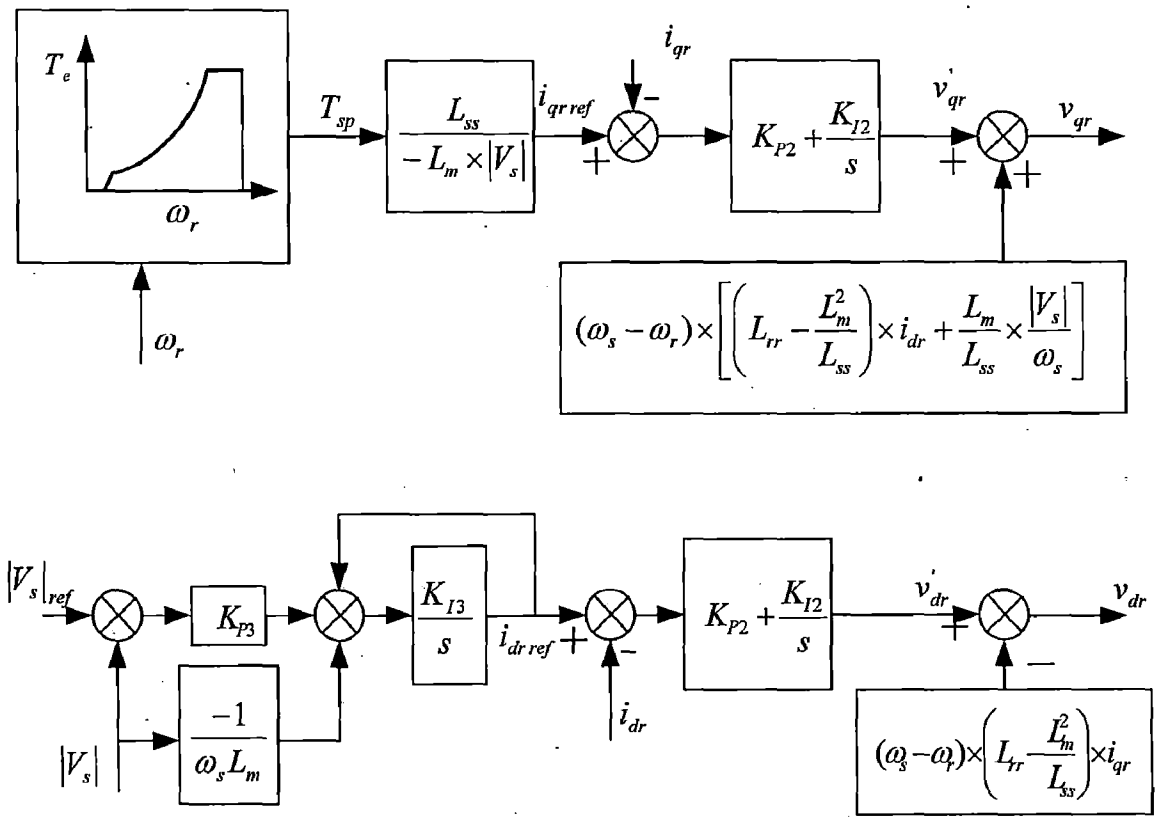

Figure 2.4: Block diagram for speed, power factor and voltage controller

v_{dr} controller equations:

$$v_{dri} - v'_{dri} + [(\omega_{si} - \omega_{ri})X_2(\frac{V_i}{\omega_{si}L_{mi}} - \frac{L_{ssi}}{L_{mi}}i_{dsi})] = 0 \quad (2.15)$$

$$\frac{di_{drefi}}{dt} = K_{I3i}[(V_i - V_{refi})K_{P3i} - \frac{V_i}{\omega_{si}L_{mi}} - i_{drefi})] \quad (2.16)$$

$$\frac{dv'_{dri}}{dt} = K_{P2i}[\frac{di_{drefi}}{dt} - \frac{1}{\omega_{si}L_{mi}}\frac{dV_i}{dt} + \frac{L_{ssi}}{L_{mi}}\frac{di_{dsi}}{dt}] + K_{I2i}[i_{drefi} - \frac{V_i}{\omega_{si}L_{mi}} + \frac{L_{ssi}}{L_{mi}}i_{dsi})] \quad (2.17)$$

v_{qr} controller equations:

$$v_{qri} - v'_{qri} - (\omega_{si} - \omega_{ri})[X_2(\frac{V_i}{\omega_{si}L_{mi}} - \frac{L_{ssi}}{L_{mi}}i_{dsi}) + \frac{L_{mi}}{L_{ssi}}\frac{V_i}{\omega_{si}}] = 0 \quad (2.18)$$

$$\frac{dv'_{qri}}{dt} = -\frac{K_{P2i}L_{ssi}}{L_{mi}}[K_{opti}\frac{d}{dt}(\frac{\omega_{ri}^2}{V_i}) + \frac{di_{qsi}}{dt}] - \frac{K_{I2i}L_{ssi}}{L_{mi}}[K_{opti}(\frac{\omega_{ri}^2}{V_i}) + i_{qsi}] \quad (2.19)$$

Where, $i = 1, 2, 3 \ldots g$

2.4 Network models

2.4.1 For Synchronous machine buses

$$I_{di}V_i\sin(\delta_i - \theta_i) + I_{qi}V_i\cos(\delta_i - \theta_i) + P_{Li}(V_i) - \sum_{k=1}^{n}V_iV_kY_{ik}\cos(\theta_i - \theta_k - \alpha_{ik}) = 0 \quad (2.20)$$

$$I_{di}V_i\cos(\delta_i - \theta_i) - I_{qi}V_i\sin(\delta_i - \theta_i) + Q_{Li}(V_i) - \sum_{k=1}^{n}V_iV_kY_{ik}\sin(\theta_i - \theta_k - \alpha_{ik}) = 0 \quad (2.21)$$

Where, $i = 1, 2, 3 \ldots m$

2.4.2 For DFIG buses

$$P_{dgi} + P_{Li} - \sum_{k=1}^{n}V_iV_kY_{ik}\cos(\theta_i - \theta_k - \alpha_{ik}) = 0 \quad (2.22)$$

$$Q_{dgi} + Q_{Li} - \sum_{k=1}^{n}V_iV_kY_{ik}\sin(\theta_i - \theta_k - \alpha_{ik}) = 0 \quad (2.23)$$

Where, $P_{dgi} = V_ii_{dsi}\cos\theta_i + V_ii_{qsi}\sin\theta_i - v_{dri}(\frac{V_i}{\omega_sL_{mi}} - \frac{L_{mi}}{L_{rri}}i_{dsi}) - \frac{L_{ssi}}{L_{mi}}i_{qsi}v_{qri}$

$$Q_{dgi} = -V_i i_{dsi}$$

Where, $i = m+1, m+2 \ldots m+g$

2.4.3 For load buses

$$P_{Li} - \sum_{k=1}^{n} V_i V_k Y_{ik} \cos(\theta_i - \theta_k - \alpha_{ik}) = 0 \quad (2.24)$$

$$Q_{Li} - \sum_{k=1}^{n} V_i V_k Y_{ik} \sin(\theta_i - \theta_k - \alpha_{ik}) = 0 \quad (2.25)$$

Where, $i = m+g+1, m+g+2 \ldots n$

2.5 Infinite Bus model

The infinite bus has been modelled as a constant frequency and constant voltage source capable of supplying any amount of load. This means that the infinite bus voltage is unaffected due to system disturbances, especially during large disturbances and is ready to supply infinite fault current.

2.6 Load model

All the loads have been modelled as constant impedance loads and remain unchanged throughout simulation. All the load dynamics have been neglected. The load impedances are included into the network Y-Bus matrix.

With the various power system elements being modeled, we now have:

With only DFIGs and infinite bus:

1. 6 differential equations for each DFIG, i.e., *6g* D.E.s.
2. 2 machine and 2 controller algebraic equations for each DFIG, i.e., *4g* algebraic equations.
3. 2 network equations each for infinite bus, DFIG buses and remaining buses, i.e., *2+2g+2(n-g-1)* equations.

Therefore, we have *6g+4g+(2+2g+2(n-g-1)) i.e., 10g+2n* Differential Algebraic Equations (DAE). From these equations the state vectors can be written as

$$x = [x_1^T \ldots . x_g^T]^T \quad ; 6g \text{ variables.} \quad (2.26)$$

$$\text{Where, } x_i = [e_{di}, e_{qi}, \omega_{ri}, i_{dr\,refi}, v'_{dri}, v'_{qri}]^T \quad (2.27)$$

The algebraic variables are

$$[vi] = [i_{dsi}, i_{qsi}, v_{dri}, v_{qri}]^T \quad ; 4g \text{ variables.} \tag{2.28}$$

$$[\bar{V}I] = [I_d, I_q, V_{i-1}\angle\theta_{i-1}]^T \quad ; 2n \text{ variables.} \tag{2.29}$$

Where,

$$[V_{i-1}] = [V_2, V_3 \ldots\ldots V_n]^T \tag{2.30}$$

$$[\theta_{i-1}] = [\theta_2, \theta_3 \ldots\ldots \theta_n]^T \tag{2.31}$$

Therefore, $10g+2n$ unknown variables.

With both DFIGs and Synchronous machines:

1. 13 differential equations, 7 for each Synchronous machine and 6 for each DFIG, i.e., $7m+6g$ D.E.s.
2. 6 algebraic equations, 2 for each Synchronous machine and 4 for each DFIG, i.e., $2m+4g$ algebraic equations.
3. 2 network equations each for DFIG buses, Synchronous machine buses and remaining buses, i.e., $2m+2g+2(n- m-g)$ equations.

Therefore, we have $7m+6g+2m+4g+(2m+2g+2(n-m-g))$ *i.e.,* $9m+10g+2n$ equations. From these equations the state vectors can be written as

$$y = [y_1^t \ldots\ldots y_m^t]^t \quad ; 7m \text{ variables.} \tag{2.32}$$

$$x = [x_1^T \ldots\ldots x_g^T]^T \quad ; 6g \text{ variables.} \tag{2.33}$$

$$\text{Where, } y_i = [E'_{qi}, E'_{qi}, \delta_i, \omega_i, E_{fdi}, R_{fi}, V_{Ri}]^T \tag{2.34}$$

$$x_i = [e_{di}, e_{qi}, \omega_{ri}, i_{dr\,refi}, v'_{dri}, v'_{qri}]^T \tag{2.35}$$

The algebraic variables are

$$[I_{dq}] = [I_{di}, I_{qi}]^T \quad ; 2m \text{ variables.} \tag{2.36}$$

$$[vi_i] = [i_{dsi}, i_{qsi}, v_{dri}, v_{qri}]^T \quad ; 4g \text{ variables.} \tag{2.37}$$

$$[\bar{V}] = [\bar{V}_i\angle\theta_i]^T \quad ; 2n \text{ variables.} \tag{2.38}$$

$$\text{Where, } [V_i] = [V_1, V_2, \ldots\ldots V_n]^T \tag{2.39}$$

$$[\theta_i] = [\theta_1, \theta_2 \ldots\ldots \theta_n]^T \tag{2.40}$$

Therefore, we have $9m+10g+2n$ unknown variables.

Using the above DAEs and solving them at each time instant, we can simulate the transient stability of the multimachine power system network with DFIG integrated into the system. There are different methods that can be used to solve these equations. However, the most commonly used method in industry for solving these equations is the "*Simultaneous Implicit (SI)*" method which is dealt in the next chapter. Also, the initial conditions required for the simulation have also been derived in the next chapter.

Chapter 3

INITIAL CONDITIONS AND SIMULATION DERIVATIONS

3.1 Initial conditions

3.1.1 Initialization of Dynamic model Initial conditions

Before the dynamic model is simulated for TSA, we need to evaluate its initial conditions. For this purpose we need to carry out the network load flow calculations. Load flow ensures that the correct operating point is achieved for the steady state conditions. Once the load flow calculations are obtained the dynamic model is ready for initialization.

For carrying out the power flow calculations, the loads, considered as constant impedance loads, were included into the network Y-Bus matrix. The infinite bus and synchronous generator buses were modelled as PV buses as they are capable of controlling the bus voltages. DFIGs on the other hand can be modelled as PV as well as PQ buses depending on whether it is controlling the terminal bus voltage or not. Fig. 3.1a and Fig. 3.1b give the sequence for initializing the dynamic model with DFIG wind turbines [12].

3.1.2 Initialization of Dynamic model

The output data of the load flow calculation is used in initializing the dynamic models of the synchronous machine and the DFIG. In case of DFIG, the initial conditions are obtained as in Fig. 3.1 which is explained in section 3.1.2.2.

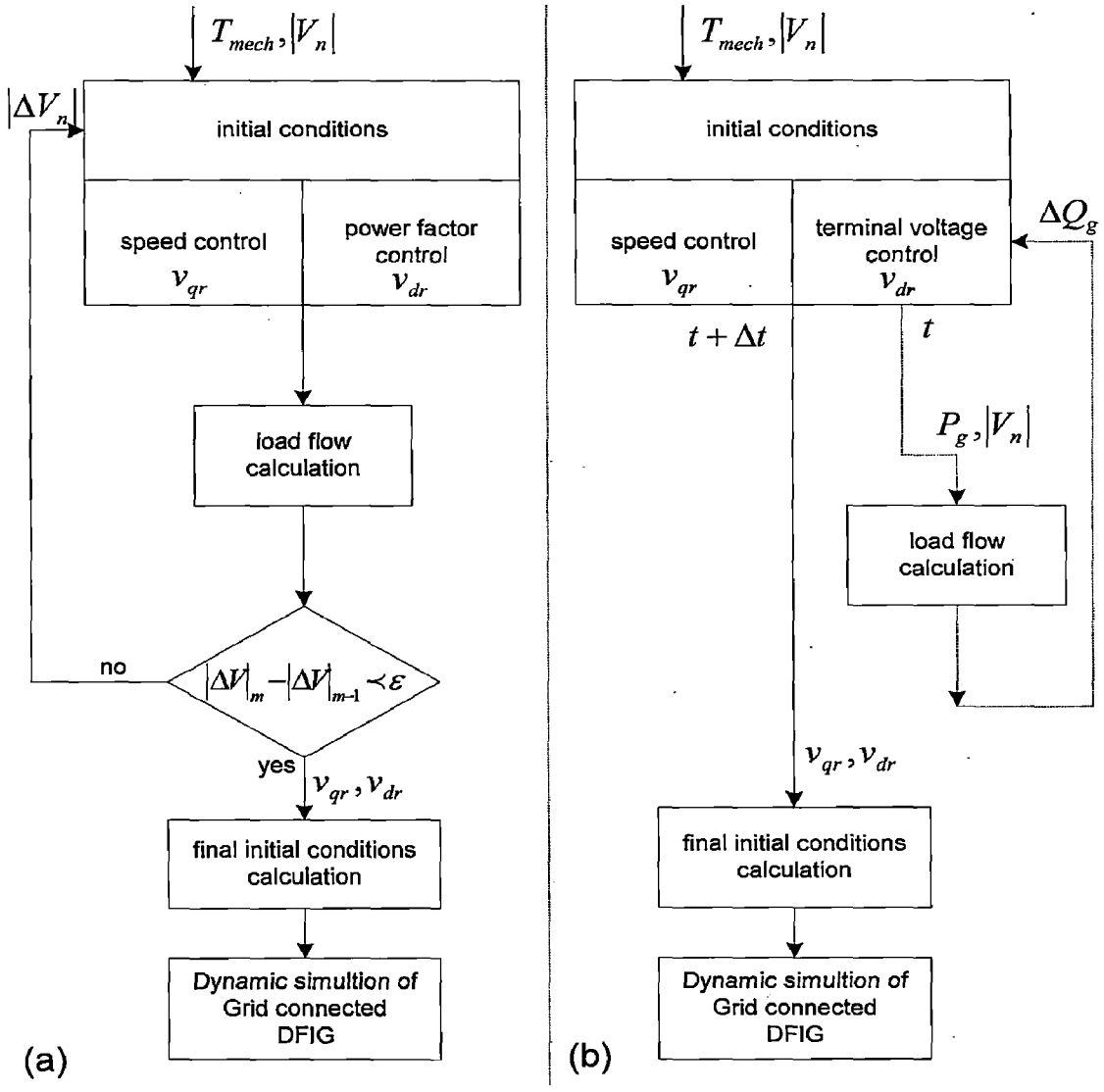

Figure 3.1: Sequence for initializing the dynamic model with DFIG wind turbines

(a) Representing DFIG model as PQ bus

(b) Representing DFIG model as PV bus

3.1.2.1 Synchronous Machine Initial conditions [15]

Following are the steps for calculating the initial conditions for synchronous machine:

Step 1: $$I_{gi}e^{j\gamma_i} = \frac{P_{gi} - jQ_{gi}}{V_i^*} \tag{3.1}$$

Step 2: $$\delta_i = \angle(V_i e^{j\theta_i} + (R_{si} - jX_{qi})I_{gi}e^{j\gamma_i} \tag{3.2}$$

Step 3: $$I_{di} + jI_{qi} = I_{gi}e^{j\gamma_i}e^{-j(\delta_i - \pi/2)} \tag{3.3}$$

$$V_{di} + jV_{qi} = V_i e^{j\gamma_i}e^{-j(\delta_i - \pi/2)} \tag{3.4}$$

Step 4: $$E'_{di} = (X_{qi} - X'_{qi})I_{qi} \quad (3.5)$$

Step 5: $$E'_{di} = V_{qi} + R_{si}I_{qi} + X'_{di}I_{di} \quad (3.6)$$

Step 6: $$E_{fdi} = E'_{qi} + (X_{di} - X'_{di})I_{qi} \quad (3.7)$$

Step 7: $$V_{Ri} = (K_{Ei} + 0.0039e^{1.555E_{fdi}})E_{fdi} \quad (3.8)$$

Step 8: $$R_{fi} = \frac{K_{Fi}}{T_{Fi}}E_{fdi} \quad (3.9)$$

Step 9: $$V_{refi} = V_i + \frac{V_{Ri}}{K_{Ai}} \quad (3.10)$$

Step 10: $$T_{Mi} = E'_{di}I_{di} + E'_{qi}I_{qi} + (X'_{qi} - X'_{di})I_{di}I_{qi} \quad (3.11)$$

Where, *i=1, 2, 3 ...m*

3.1.2.2 DFIG Initial Conditions

As DFIG is capable of supplying reactive power and controlling the terminal voltage, DFIG bus can be considered as a PV bus. But since the DFIG, when integrated with the grid, is not strong enough to control the Grid voltage and hence the reactive power, in this dissertation work, it has been considered as a PQ bus [9].

Setting all the differential terms in DFIG dynamic model to zero [13] and following the procedure given in Fig. 3.1a, following steps have been derived for calculating initial conditions for DFIG as a PQ bus.

Step 1:

$$X_i = X_{si} + X_{mi}$$

$$L_{si} = X_{si}/\omega_{si} \qquad L_{ri} = X_{ri}/\omega_{si} \qquad L_{mi} = X_{mi}/\omega_{si}$$

$$L_{ssi} = L_{si} + L_{mi} \qquad L_{rri} = L_{ri} + L_{mi}$$

$$X'_i = \omega_{si}(L_{ssi} - \frac{L_{mi}^2}{L_{rri}}) \qquad X_{2i} = (L_{rri} - \frac{L_{mi}^2}{L_{ssi}}) \qquad T_{oi} = (\frac{L_{ri} + L_{mi}}{R_{ri}}) \quad (3.12)$$

Step 2: $$\omega_{ri} = (\frac{T_{mi}}{K_{opti}})^{1/2} \qquad s_i = (\frac{\omega_{si} - \omega_{ri}}{\omega_{si}}) \quad (3.13)$$

Step 3: $$v_{dsi} = real(V_i e^{j\theta_i}) \qquad v_{qsi} = img(V_i e^{j\theta_i}) \quad (3.14)$$

Step 4: $$i_{dsi} = \frac{2V_i}{\omega_{si}L_{ssi}} \qquad i_{qsi} = \frac{-K_{opti}\omega_{ri}^2}{V_i} \quad (3.15)$$

Step 5: $$i_{dri} = (\frac{V_i}{\omega_{si} L_{mi}} - \frac{L_{ssi}}{L_{mi}} i_{dsi}) \qquad i_{dri} = \frac{L_{ssi}}{L_{mi}} i_{qsi} \tag{3.16}$$

Step 6: $$i_{dr\,refi} = -\frac{V_i}{\omega_{si} L_{mi}} \tag{3.17}$$

Step 7: $$e_{di} = V_i \cos\theta_i + R_{si} i_{dsi} - X_i^{'} i_{qsi}$$

$$e_{qi} = V_i \sin\theta_i + X_i^{'} i_{dsi} + R_{si} i_{qsi} \tag{3.18}$$

Step 8: $$v_{dri} = [\frac{1}{T_{oi}}(e_{qi} + (X_i - X_i^{'}) i_{dsi}) + s_i \omega_s e_{di}] \frac{L_{rri}}{\omega_{si} L_{mi}}$$

$$v_{qri} = [-\frac{1}{T_{oi}}(e_{di} - (X_i - X_i^{'}) i_{qsi}) + s \omega_s e_{qi}] \frac{L_{rri}}{\omega_{si} L_{mi}} \tag{3.19}$$

Step 9: $$P_{dgi} = V_i i_{dsi} \cos\theta_i + V_i i_{qsi} \sin\theta_i - v_{dri} (\frac{V_i}{\omega_s L_{mi}} - \frac{L_{mi}}{L_{rri}} i_{dsi}) - \frac{L_{ssi}}{L_{mi}} i_{qsi} v_{qri}$$

$$Q_{dgi} = -V_i i_{dsi} \tag{3.20}$$

Where, $i=1, 2, 3 \ldots g$

Step 10: Carryout load flow calculation. Repeat Steps 3 to 10 till change in voltage error is less than the specified error ε.

Step 11: $$v_{dri}^{'} = v_{dri} + [(\omega_{si} - \omega_{ri}) X_2 (\frac{V_i}{\omega_{si} L_{mi}} - \frac{L_{ssi}}{L_{mi}} i_{dsi})]$$

$$v_{qri}^{'} = v_{qri} - (\omega_{si} - \omega_{ri}) [X_2 (\frac{V_i}{\omega_{si} L_{mi}} - \frac{L_{ssi}}{L_{mi}} i_{dsi}) + \frac{L_{mi}}{L_{ssi}} \frac{V_i}{\omega_{si}}] \tag{3.21}$$

3.2 SI method

3.2.1 General method [15]

In this particular section the basic procedure of SI method will be discussed and later its application to Transient Stability Analysis (TSA) will be explained.

In SI method, first the differential equations are converted to algebraic equations and the resulting algebraic equations along with the other algebraic equations are solved simultaneously using the Newton's method at each time step.

Let, $\dot{x}$ be a set consisting of differential equations and g_o be a set of algebraic equations. Say, $\dot{x} = f_o(x, y)$ which is converted to algebraic equations using either the

trapezoidal integration method or the implicit Euler's method. In this dissertation, the trapezoidal integration method has been used which is as given below:

$$\dot{x} = f_o(x, y) \tag{3.22}$$

$$\int_{t_n}^{t_{n+1}} \dot{x}dt = \int_{t_n}^{t_{n+1}} f_o(x, y)dt \tag{3.23}$$

$$x_{n+1} = x_n + \frac{\Delta t}{2}[f_o(x_{n+1}, y_{n+1}) + f_o(x_n, y_n)] \tag{3.24}$$

$$0 = g_o(x_{n+1}, y_{n+1}) \tag{3.25}$$

($n+1$ and n denoting the time instants t_{n+1} and t_n respectively)

These algebraic equations are then solved at each time step using the Newton's method.

3.2.2 Application to TSA

For multimachine TSA using SI method, the trapezoidal integration method has been applied to DAEs presented in the previous chapter. The resulting algebraic equations are solved simultaneously using the Newton's method. This process is carried out for each time step till the end of the simulation. For TSA a fault is applied on one of the buses at a particular time instant and then the response of the system is observed. Fig. 3.2 shows flow chart for TSA using SI-method.

3.2.3 Trapezoidal Integration Method

Let us denote the superscripts $n+1$ and n as time instants t_{n+1} and t_n respectively. Then using the trapezoidal method for each time instant we can derive the required algebraic equations as:

3.2.3.1 For Synchronous Machines

1. We have,

$$T'_{doi}\frac{dE'_{qi}}{dt} = -E'_{qi} - (X_{di} - X'_{di})I_{di} + E_{fdi}$$

Rearranging the above equation,

$$\frac{dE'_{qi}}{dt} = \frac{1}{T'_{doi}}[-E'_{qi} - (X_{di} - X'_{di})I_{di} + E_{fdi}] \tag{3.26}$$

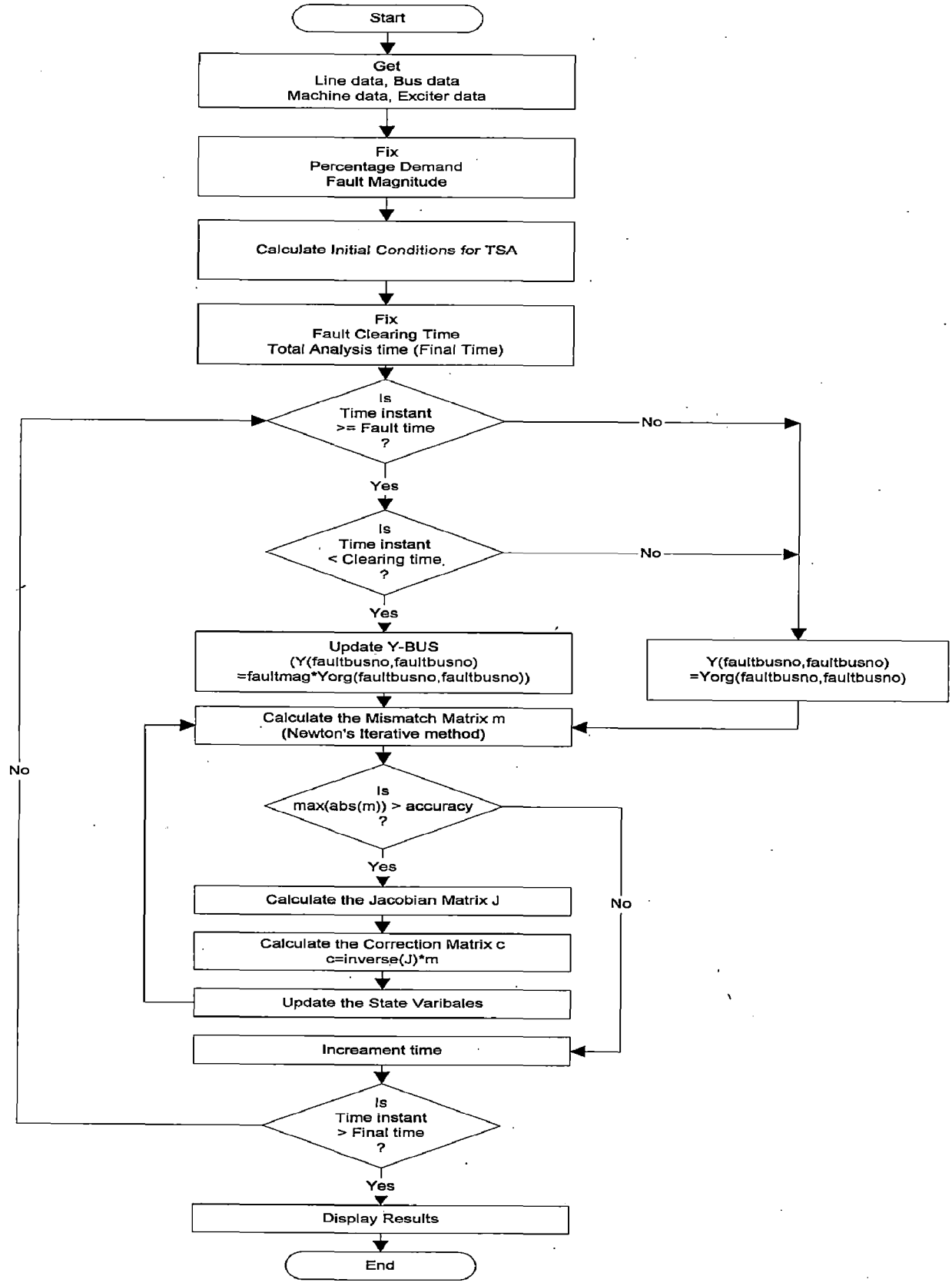

Figure 3.2: Flow chart for TSA using SI-method

Using the trapezoidal integration,

$$E_{qi}^{',n+1} = E_{qi}^{',n} + \frac{\Delta t}{2T_{doi}^{'}}[-E_{qi}^{',n+1} - (X_{di} - X_{di}^{'})I_{di}^{n+1} + E_{fdi}^{n+1} - E_{qi}^{',n} - (X_{di} - X_{di}^{'})I_{di}^{n} + E_{fdi}^{n}]$$

$$E_{qi}^{',n+1}(1 + \frac{\Delta t}{2T_{doi}^{'}}) + \frac{\Delta t}{2T_{doi}^{'}}[(X_{di} - X_{di}^{'})I_{di}^{n+1} - E_{fdi}^{n+1}] = f_1^n \quad (3.27)$$

Where,

$$f_1^n = E_{qi}^{',n}(1 - \frac{\Delta t}{2T_{doi}^{'}}) + \frac{\Delta t}{2T_{doi}^{'}}[-(X_{di} - X_{di}^{'})I_{di}^{n} + E_{fdi}^{n}] \quad (3.28)$$

In a similar manner for other equations we have as follows.

2. $$T_{qoi}^{'}\frac{dE_{di}^{'}}{dt} = -E_{di}^{'} - (X_{qi} - X_{qi}^{'})I_{qi}$$

$$E_{di}^{',n+1}(1 + \frac{\Delta t}{2T_{qoi}^{'}}) - \frac{\Delta t}{2T_{qoi}^{'}}(X_{qi} - X_{qi}^{'})I_{qi}^{n+1} = f_2^n \quad (3.29)$$

$$f_2^n = E_{di}^{',n}(1 - \frac{\Delta t}{2T_{qoi}^{'}}) + \frac{\Delta t}{2T_{qoi}^{'}}(X_{qi} - X_{qi}^{'})I_{qi}^{n} \quad (3.30)$$

3. $$\frac{d\delta_i}{dt} = (\omega_i - \omega_s)$$

$$\delta_i^{n+1} - \frac{\Delta t}{2}\omega_i^{n+1} = f_3^n \quad (3.31)$$

$$f_3^n = \delta_i^n + \frac{\Delta t}{2}(\omega_i^n - 2\omega_s) \quad (3.32)$$

4. $$\frac{2H_i}{\omega_s}\frac{d\omega_i}{dt} = T_{Mi} - E_{di}^{'}I_{di} - E_{di}^{'}I_{di} - (X_{qi}^{'} - X_{di}^{'})I_{di}I_{qi} - D_i(\omega_i - \omega_s)$$

$$\omega_i^{n+1}(1 + \frac{\Delta t}{2}\frac{\omega_s D_i}{2H_i}) + \frac{\Delta t}{2}\frac{\omega_s}{2H_i}[E_{qi}^{n+1}I_{qi}^{n+1} + E_{di}^{n+1}I_{qi}^{n+1} + (X_{qi}^{'} - X_{di}^{'})I_{di}^{n+1}I_{qi}^{n+1}] = f_4^n$$

(3.33)

$$f_4^n = \omega_i^n(1 - \frac{\Delta t}{2}\frac{\omega_s D_i}{2H_i}) + \frac{\Delta t}{2}\frac{\omega_s}{2H_i}[2T_{Mi} + 2D_i - E_{qi}^{n}I_{qi}^{n} - E_{di}^{n}I_{qi}^{n} - (X_{qi}^{'} - X_{di}^{'})I_{di}^{n}I_{qi}^{n}]$$

(3.34)

5. $$T_{Ei}\frac{dE_{fdi}}{dt} = -(K_{Ei} + S_{Ei}(E_{fdi}))E_{fdi} + V_{Ri}$$

$$E_{fdi}^{n+1}[1+\frac{\Delta t}{2T_{Ei}}(K_{Ei}+S_{Ei}(E_{fdi}^{n+1}))]-\frac{\Delta t}{2T_{Ei}}V_{Ri}^{n+1}=f_5^n \tag{3.35}$$

$$f_5^n = E_{fdi}^n[1-\frac{\Delta t}{2T_{Ei}}(K_{Ei}+S_{Ei}(E_{fdi}^n))]+\frac{\Delta t}{2T_{Ei}}V_{Ri}^n \tag{3.36}$$

6. $$T_{Fi}\frac{dR_{fi}}{dt}=-R_{fi}+\frac{K_{Fi}}{T_{Fi}}E_{fdi}$$

$$R_{fi}^{n+1}(1+\frac{\Delta t}{2T_{Fi}})-\frac{\Delta t}{2T_{Fi}}\frac{K_{Fi}}{T_{Fi}}E_{fdi}^{n+1}=f_6^n \tag{3.37}$$

$$f_6^n = R_{fi}^n(1-\frac{\Delta t}{2T_{Fi}})+\frac{\Delta t}{2T_{Fi}}\frac{K_{Fi}}{T_{Fi}}E_{fdi}^n \tag{3.38}$$

7. $$T_{Ai}\frac{dV_{Ri}}{dt}=-V_{Ri}+K_{Ai}R_{fi}-\frac{K_{Ai}K_{Fi}}{T_{Fi}}E_{fdi}+K_{Ai}(V_{refi}-V_i)$$

$$V_{Ri}^{n+1}(1+\frac{\Delta t}{2T_{Ai}})-\frac{\Delta t}{2T_{Ai}}K_{Ai}[R_{fi}^{n+1}-\frac{K_{Fi}}{T_{Fi}}E_{fdi}^{n+1}-V_i^{n+1}]=f_7^n \tag{3.39}$$

$$f_7^n = V_{Ri}^n(1-\frac{\Delta t}{2T_{Ai}})+\frac{\Delta t}{2T_{Ai}}K_{Ai}[R_{fi}^n-\frac{K_{Fi}}{T_{Fi}}E_{fdi}^n-V_i^n+2V_{refi}] \tag{3.40}$$

8. $$E_{di}^{'}-V_i\sin(\delta_i-\theta_i)-R_{Si}I_{di}+X_{qi}^{'}I_{qi}=0$$

$$V_i^{n+1}\sin(\delta_i^{n+1}-\theta_i^{n+1})-X_{qi}^{'}I_{qi}^{n+1}-E_{di}^{',n+1}=f_8^n \tag{3.41}$$

$$f_8^n = 0 \tag{3.42}$$

9. $$E_{qi}^{'}-V_i\cos(\delta_i-\theta_i)-R_{Si}I_{qi}-X_{di}^{'}I_{di}=0$$

$$V_i^{n+1}\cos(\delta_i^{n+1}-\theta_i^{n+1})+X_{di}^{'}I_{di}^{n+1}-E_{qi}^{',n+1}=f_9^n \tag{3.43}$$

$$f_9^n = 0 \tag{3.44}$$

3.2.3.2 For DFIGs

1. $$-R_{si}i_{dsi}+X_i^{'}i_{qsi}+e_{di}-V_i\cos\theta_i=0$$

$$-R_{si}i_{dsi}^{n+1}+X_i^{'}i_{qsi}^{n+1}+e_{di}^{n+1}-V_i^{n+1}\cos\theta_i^{n+1}=g_1^n \tag{3.45}$$

$$g_1^n=0 \tag{3.46}$$

2. $$-R_{si}i_{qsi}-X_i^{'}i_{dsi}+e_{qi}-V_i\sin\theta_i=0$$

$$-R_{si}i_{qsi}^{n+1}-X_i^{'}i_{dsi}^{n+1}+e_{di}^{n+1}-V_i^{n+1}\sin\theta_i^{n+1}=g_2^n \tag{3.47}$$

$$g_2^n=0 \tag{3.48}$$

3.

$$\frac{de_{di}}{dt} = -\frac{1}{T_{oi}}[e_{di} - (X_i - X_i^{'})i_{qsi}] + s\omega_s e_{qi} - \omega_s \frac{L_{mi}}{L_{rri}} v_{qri}$$

$$e_{di}^{n+1} - \frac{\Delta t}{2}\left\{-\frac{1}{T_{oi}}[e_{di}^{n+1} - (X_i - X_i^{'})i_{qsi}^{n+1}] + s_i^{n+1}\omega_s e_{qi}^{n+1} - \omega_s \frac{L_{mi}}{L_{rri}} v_{qri}^{n+1}\right\} = g_3^n \quad (3.49)$$

$$g_3^n = e_{di}^{n+1} + \frac{\Delta t}{2}\left\{-\frac{1}{T_{oi}}[e_{di}^{n} - (X_i - X_i^{'})i_{qsi}^{n}] + s_i^{n}\omega_s e_{qi}^{n} - \omega_s \frac{L_{mi}}{L_{rri}} v_{qri}^{n}\right\} \quad (3.50)$$

4.

$$\frac{de_{qi}}{dt} = -\frac{1}{T_{oi}}[e_{qi} + (X_i - X_i^{'})i_{dsi}] - s\omega_s e_{di} + \omega_s \frac{L_{mi}}{L_{rri}} v_{dri}$$

$$e_{qi}^{n+1} - \frac{\Delta t}{2}\left\{-\frac{1}{T_{oi}}[e_{qi}^{n+1} + (X_i - X_i^{'})i_{dsi}^{n+1}] - s_i^{n+1}\omega_s e_{di}^{n+1} + \omega_s \frac{L_{mi}}{L_{rri}} v_{dri}^{n+1}\right\} = g_4^n \quad (3.51)$$

$$g_4^n = e_{qi}^{n} + \frac{\Delta t}{2}\left\{-\frac{1}{T_{oi}}[e_{qi}^{n} + (X_i - X_i^{'})i_{dsi}^{n}] - s_i^{n}\omega_s e_{di}^{n} + \omega_s \frac{L_{mi}}{L_{rri}} v_{dri}^{n}\right\} \quad (3.52)$$

5.

$$\frac{d\omega_{ri}}{dt} = \frac{1}{2H_{ti}}\left[T_{mi} + \frac{V_i i_{qsi}}{\omega_{si}}\right]$$

$$\omega_{ri}^{n+1} - \frac{\Delta t}{4H_{ti}}\frac{V_i^{n+1} i_{qsi}^{n+1}}{\omega_{si}} = g_5^n \quad (3.53)$$

$$g_5^n = \omega_{ri}^{n} + \frac{\Delta t}{4H_{ti}}\left[2T_{mi} + \frac{V_i^{n} i_{qsi}^{n}}{\omega_{si}}\right] \quad (3.54)$$

6.

$$v_{dri} - v_{dri}^{'} + \left[(\omega_{si} - \omega_{ri})X_2\left(\frac{V_i}{\omega_{si}L_{mi}} - \frac{L_{ssi}}{L_{mi}} i_{dsi}\right)\right] = 0$$

$$v_{dri}^{n+1} - v_{dri}^{'n+1} + \left[(\omega_{si} - \omega_{ri}^{n+1})X_2\left(\frac{V_i^{n+1}}{\omega_{si}L_{mi}} - \frac{L_{ssi}}{L_{mi}} i_{dsi}^{n+1}\right)\right] = g_6^n \quad (3.55)$$

$$g_6^n = 0 \quad (3.56)$$

7.

$$\frac{di_{drrefi}}{dt} = K_{I3i}\left[(V_i - V_{refi})K_{P3i} - \frac{V_i}{\omega_{si}L_{mi}} - i_{drrefi}\right]$$

$$\left(1 + \frac{\Delta t}{2}K_{I3i}\right)i_{drrefi}^{n+1} - \frac{\Delta t}{2}K_{I3i}\left(K_{p3i} - \frac{1}{\omega_{si}L_{mi}}\right)V_i^{n+1} = g_7^n \quad (3.57)$$

$$g_7^n = \left(1 - \frac{\Delta t}{2} K_{I3i}\right) i_{drrefi}^n + \frac{\Delta t}{2} K_{I3i} \left(K_{p3i} - \frac{1}{\omega_{si} L_{mi}}\right) V_i^n - \frac{\Delta t}{2} K_{P3i} K_{I3i} V_{refi} \quad (3.58)$$

8. $$\frac{d v'_{dri}}{dt} = K_{P2i}\left[\frac{di_{dr\,refi}}{dt} - \frac{1}{\omega_{si} L_{mi}} \frac{dV_i}{dt} + \frac{L_{ssi}}{L_{mi}} \frac{di_{dsi}}{dt}\right] + K_{I2i}\left[i_{dr\,refi} - \frac{V_i}{\omega_{si} L_{mi}} + \frac{L_{ssi}}{L_{mi}} i_{dsi}\right]$$

$$v'^{n+1}_{dri} - \left(K_{P2i} + \frac{\Delta t}{2} K_{I2i}\right)\left[i^{n+1}_{dr\,refi} - \frac{V_i^{n+1}}{\omega_{si} L_{mi}} + \frac{L_{ssi}}{L_{mi}} i^{n+1}_{dsi}\right] = g_8^n \quad (3.59)$$

$$g_8^n = v'^{n}_{dri} - \left(K_{P2i} - \frac{\Delta t}{2} K_{I2i}\right)\left[i^{n}_{dr\,refi} - \frac{V_i^{n}}{\omega_{si} L_{mi}} + \frac{L_{ssi}}{L_{mi}} i^{n}_{dsi}\right] \quad (3.60)$$

9. $$v_{qri} - v'_{qri} - (\omega_{si} - \omega_{ri})\left[X_2\left(\frac{V_i}{\omega_{si} L_{mi}} - \frac{L_{ssi}}{L_{mi}} i_{dsi}\right) + \frac{L_{mi}}{L_{ssi}} \frac{V_i}{\omega_{si}}\right] = 0$$

$$v^{n+1}_{qri} - v'^{n+1}_{qri} - (\omega_{si} - \omega^{n+1}_{ri})\left[X_2\left(\frac{V_i^{n+1}}{\omega_{si} L_{mi}} - \frac{L_{ssi}}{L_{mi}} i^{n+1}_{dsi}\right) + \frac{L_{mi}}{L_{ssi}} \frac{V_i^{n+1}}{\omega_{si}}\right] = g_9^n \quad (3.61)$$

$$g_9^n = 0 \quad (3.62)$$

10. $$\frac{d v'_{qri}}{dt} = -\frac{K_{P2i} L_{ssi}}{L_{mi}}\left[K_{opti} \frac{d}{dt}\left(\frac{\omega_{ri}^2}{V_i}\right) + \frac{di_{qsi}}{dt}\right] - \frac{K_{I2i} L_{ssi}}{L_{mi}}\left[K_{opti}\left(\frac{\omega_{ri}^2}{V_i}\right) + i_{qsi}\right]$$

$$v'^{n+1}_{qri} + \left(K_{P2i} + \frac{\Delta t}{2} K_{I2i}\right)\frac{L_{ssi}}{L_{mi}}\left[K_{opti} \frac{\omega_{ri}^{2,n+1}}{V_i^{n+1}} + i^{n+1}_{qsi}\right] = g_{10}^n \quad (3.63)$$

$$g_{10}^n = v'^{n}_{qri} + \left(K_{P2i} - \frac{\Delta t}{2} K_{I2i}\right)\frac{L_{ssi}}{L_{mi}}\left[K_{opti} \frac{\omega_{ri}^{2,n}}{V_i^{n}} + i^{n}_{qsi}\right] \quad (3.64)$$

3.2.3.3 Network equations for Synchronous machine bus and infinite bus

In this case, eqns. (3.65 - 3.68) can be used for infinite bus as well as synchronous machine bus. For an infinite bus, the corresponding differential eqns. would be omitted from simulation and the terminal voltage magnitudes and angles would have some specified value. In case of synchronous machines, eqns. (3.65 - 3.68) remain unchanged.

1. $$I_{di} V_i \sin(\delta_i - \theta_i) + I_{qi} V_i \cos(\delta_i - \theta_i) + P_{Li}(V_i) - \sum_{k=1}^{n} V_i V_k Y_{ik} \cos(\theta_i - \theta_k - \alpha_{ik}) = 0$$

$$\sum_{k=1}^{n} V_i^{n+1} V_k^{n+1} Y_{ik} \cos(\theta_i^{n+1} - \theta_k^{n+1} - \alpha_{ik}) - I_{di}^{n+1} V_i^{n+1} \sin(\delta_i^{n+1} - \theta_i^{n+1}) \ldots$$

$$- I_{qi}^{n+1} V_i^{n+1} \cos(\delta_i^{n+1} - \theta_i^{n+1}) = h_1^n \quad (3.65)$$

$$h_1^n = 0 \tag{3.66}$$

2. $I_{di}V_i\cos(\delta_i-\theta_i)-I_{qi}V_i\sin(\delta_i-\theta_i)-\sum_{k=1}^{n}V_iV_kY_{ik}\sin(\theta_i-\theta_k-\alpha_{ik})=0$

$$\sum_{k=1}^{n}V_i^{n+1}V_k^{n+1}Y_{ik}\sin(\theta_i^{n+1}-\theta_k^{n+1}-\alpha_{ik})-I_{di}^{n+1}V_i^{n+1}\cos(\delta_i^{n+1}-\theta_i^{n+1})\ldots$$

$$+I_{qi}^{n+1}V_i^{n+1}\sin(\delta_i^{n+1}-\theta_i^{n+1})=h_2^n \tag{3.67}$$

$$h_2^n = 0 \tag{3.68}$$

Where, $i = 1, 2 \ldots m$

3.2.3.4 Network equations for DFIG buses

3. $V_i i_{dsi}\cos\theta_i + V_i i_{qsi}\sin\theta_i - v_{dri}\left(\frac{V_i}{\omega_s L_{mi}} - \frac{L_{mi}}{L_{rri}}i_{dsi}\right) - \frac{L_{ssi}}{L_{mi}}i_{qsi}v_{qri} + P_{Li}\ldots$

$$-\sum_{k=1}^{n}V_iV_kY_{ik}\cos(\theta_i-\theta_k-\alpha_{ik})=0$$

$$V_i^{n+1}i_{dsi}^{n+1}\cos\theta_i + V_i^{n+1}i_{qsi}^{n+1}\sin\theta_i - v_{dri}^{n+1}\left(\frac{V_i^{n+1}}{\omega_s L_{mi}} - \frac{L_{mi}}{L_{rri}}i_{dsi}^{n+1}\right) - \frac{L_{ssi}}{L_{mi}}v_{qri}^{n+1}i_{qsi}^{n+1}\ldots$$

$$-\sum_{k=1}^{n}V_i^{n+1}V_k^{n+1}Y_{ik}\cos(\theta_i^{n+1}-\theta_k^{n+1}-\alpha_{ik})=h_3^n \tag{3.69}$$

$$h_3^n = 0 \tag{3.70}$$

4. $-V_i i_{dsi} - \sum_{k=1}^{n}V_iV_kY_{ik}\sin(\theta_i-\theta_k-\alpha_{ik})=0$

$$V_i^{n+1}i_{dsi}^{n+1} - \sum_{k=1}^{n}V_i^{n+1}V_k^{n+1}Y_{ik}\sin(\theta_i^{n+1}-\theta_k^{n+1}-\alpha_{ik})=h_4^n \tag{3.71}$$

$$h_4^n = 0 \tag{3.72}$$

Where, $i = m+1, m+2 \ldots m+g$

3.2.3.5 Network equations for load buses

5. $-\sum_{k=1}^{n}V_iV_kY_{ik}\cos(\theta_i-\theta_k-\alpha_{ik})=0$

$$-\sum_{k=1}^{n}V_i^{n+1}V_k^{n+1}Y_{ik}\cos(\theta_i^{n+1}-\theta_k^{n+1}-\alpha_{ik})=h_5^n \tag{3.73}$$

$$h_5^n = 0 \tag{3.74}$$

6. $$-\sum_{k=1}^{n} V_i V_k Y_{ik} \sin(\theta_i - \theta_k - \alpha_{ik}) = 0$$

$$-\sum_{k=1}^{n} V_i^{n+1} V_k^{n+1} Y_{ik} \sin(\theta_i^{n+1} - \theta_k^{n+1} - \alpha_{ik}) = h_6^n \tag{3.75}$$

$$h_6^n = 0 \tag{3.76}$$

3.3 Newton's iterative method

The above equations derived by trapezoidal integration method are solved using the Newton's iterative method for each time instant and the procedure is as given below:

$$\Delta c = [J]^{-1} \Delta m \tag{3.77}$$

Where,

$\Delta c =$ Correction matrix

$\Delta m =$ Mismatch matrix

$[J] =$ Jacobian matrix

In case of DFIGs and Synchronous machines in the network:

$$\Delta c = [\Delta E_q^{'}, \Delta E_q^{'}, \Delta\delta, \Delta\omega, \Delta E_{fd}, \Delta R_f, \Delta V_R, \Delta I_d, \Delta I_q, \Delta i_{dsi}, \Delta i_{qsi}, \Delta e_{di}, \Delta e_{qi}, \ldots.$$

$$\Delta\omega_{ri}, \Delta v_{dri}, \Delta i_{dr\,refi}, \Delta v_{dri}^{'}, \Delta v_{qri}, \Delta v_{qri}^{'}, \Delta V, \Delta\theta]^T_{((9m+10g+2n)\times 1)} \tag{3.78}$$

$$\Delta m = [\Delta f_1, \Delta f_2, \ldots \Delta f_9, \Delta g_1, \Delta g_2, \ldots \Delta g_{10}, \Delta h_1, \Delta h_2, \ldots \Delta h_6]^T_{((9m+10g+2n)\times 1)} \tag{3.79}$$

$$[J] = \begin{bmatrix} J_1 & \cdots & \cdots & \cdots & J_{21} \\ \vdots & \ddots & & & \vdots \\ \vdots & & \ddots & & \vdots \\ \vdots & & & \ddots & \vdots \\ J_{421} & \cdots & \cdots & \cdots & J_{431} \end{bmatrix}_{(9m+10g+2n)\times(9m+10g+2n)} \tag{3.80}$$

In case of DFIGs and infinite bus in the network:

$$\Delta c = [\Delta i_{dsi}, \Delta i_{qsi}, \Delta e_{di}, \Delta e_{qi}, \Delta\omega_{ri}, \Delta v_{dri}, \Delta i_{dr\,refi}, \Delta v_{dri}^{'}, \Delta v_{qri}, \Delta v_{qri}^{'}, \ldots$$

$$\Delta I_d, \Delta I_q, \Delta V_{i-1}, \Delta\theta_{i-1}]^T_{((10g+2n)\times 1)} \tag{3.81}$$

$$\Delta m = [\Delta g_1, \Delta g_2, \ldots \Delta g_{10}, \Delta h_1, \Delta h_2, \ldots \Delta h_6]^T_{((10g+2n)\times 1)} \tag{3.82}$$

$$[J]=\begin{bmatrix} J_1 & \cdots & \cdots & \cdots & J_{14} \\ \vdots & \ddots & & & \vdots \\ \vdots & & \ddots & & \vdots \\ \vdots & & & \ddots & \vdots \\ J_{211} & \cdots & \cdots & \cdots & J_{224} \end{bmatrix}_{(10g+2n)\times(10g+2n)} \tag{3.83}$$

3.3.1 Derivation of Jacobian Elements

In this section, the jacobian elements for the above mentioned cases have been derived. These derivations have been divided into three parts. In the first and second part jacobian elements related to synchronous machines and DFIGs have been derived. In the third part, jacobian elements related to network equations, which include network equations for synchronous machines buses, DFIG buses, infinite bus and remaining buses, have been derived. The jacobian subscript notations numbered in the following derivations of the above mentioned three parts are independent to each other and only non-zero terms have been presented.

Part 1: Synchronous machines

$\Delta f_1 \leftrightarrow E'_{qi}, I_{di}, E_{fdi}$:

$$J_1:(\text{m x m}):\ \frac{\partial f_1}{\partial E'_q} \quad : J_1(i,i)=(1+\frac{\Delta t}{2T'_{doi}}) \tag{3.84}$$

$$J_5:(\text{m x m}):\ \frac{\partial f_1}{\partial E_{fd}} \quad : J_5(i,i)=-\frac{\Delta t}{2T'_{doi}} \tag{3.85}$$

$$J_8:(\text{m x m}):\ \frac{\partial f_1}{\partial I_d} \quad : J_8(i,i)=\frac{\Delta t}{2T'_{doi}}(X_{di}-X'_{di}) \tag{3.86}$$

$\Delta f_2 \leftrightarrow E'_d, I_q$:

$$J_2:(\text{m x m}):\ \frac{\partial f_2}{\partial E'_d} \quad : J_2(i,i)=(1+\frac{\Delta t}{2T'_{qoi}}) \tag{3.87}$$

$$J_9:(\text{m x m}):\ \frac{\partial f_2}{\partial I_q} \quad : J_9(i,i)=-\frac{\Delta t}{2T'_{qoi}}(X_{qi}-X'_{qi}) \tag{3.88}$$

$\Delta f_3 \leftrightarrow \delta, \omega$:

$$J_3:(\text{m x m}):\ \frac{\partial f_3}{\partial \delta} \quad : J_3(i,i)=1 \tag{3.89}$$

$$J_4:(\text{m x m}):\ \frac{\partial f_3}{\partial \omega}\quad :J_4(i,i)=-\frac{\Delta t}{2} \tag{3.90}$$

$\underline{\Delta f_4 \leftrightarrow E_q^{'}, E_d^{'}, \omega, I_d, I_q}$:

$$J_1:(\text{m x m}):\ \frac{\partial f_4}{\partial E_q^{'}}\quad :J_1(i,i)=\frac{\Delta t}{4H}\omega_S I_{qi} \tag{3.91}$$

$$J_2:(\text{m x m}):\ \frac{\partial f_4}{\partial E_d^{'}}\quad :J_2(i,i)=\frac{\Delta t}{4H}\omega_S I_{di} \tag{3.92}$$

$$J_4:(\text{m x m}):\ \frac{\partial f_4}{\partial \omega}\quad :J_4(i,i)=(1+\frac{\Delta t}{4H}\omega_S D_i) \tag{3.93}$$

$$J_8:(\text{m x m}):\ \frac{\partial f_4}{\partial I_d}\quad :J_8(i,i)=\frac{\Delta t}{4H}\omega_S[E_{di}^{'}+(X_{qi}^{'}-X_{di}^{'})I_{qi}] \tag{3.94}$$

$$J_9:(\text{m x m}):\ \frac{\partial f_4}{\partial I_q}\quad :J_9(i,i)=\frac{\Delta t}{4H}\omega_S[E_{qi}^{'}+(X_{qi}^{'}-X_{di}^{'})I_{di}] \tag{3.95}$$

$\underline{\Delta f_5 \leftrightarrow E_{fd}, V_R}$:

$$J_5:(\text{m x m}):\ \frac{\partial f_5}{\partial E_{fd}}\quad :J_5(i,i)=1+\frac{\Delta t}{2T_{Ei}}[K_{Ei}+S_{Ei}(E_{fdi})\{1+E_{fdi}\}] \tag{3.96}$$

$$J_7:(\text{m x m}):\ \frac{\partial f_5}{\partial V_R}\quad :J_7(i,i)=-\frac{\Delta t}{2T_{Ei}} \tag{3.97}$$

$\underline{\Delta f_6 \leftrightarrow E_{fd}, R_f}$:

$$J_5:(\text{m x m}):\ \frac{\partial f_6}{\partial E_{fd}}\quad :J_5(i,i)=-\frac{\Delta t}{2T_{Fi}}\frac{K_{Fi}}{T_{Fi}} \tag{3.98}$$

$$J_6:(\text{m x m}):\ \frac{\partial f_6}{\partial R_f}\quad :J_6(i,i)=(1+\frac{\Delta t}{2T_{Fi}}) \tag{3.99}$$

$\underline{\Delta f_7 \leftrightarrow E_{fd}, R_f, V_R, V}$:

$$J_5:(\text{m x m}):\ \frac{\partial f_7}{\partial E_{fd}}\quad :J_5(i,i)=\frac{\Delta t}{2T_{Ai}}\frac{K_{Ai}K_{Fi}}{T_{Fi}} \tag{3.100}$$

$$J_6:(\text{m x m}):\ \frac{\partial f_7}{\partial R_f}\quad :J_6(i,i)=-\frac{\Delta t}{2T_{Ai}}K_{Ai} \tag{3.101}$$

$$J_7:(\text{m x m}):\ \frac{\partial f_7}{\partial V_R}\quad :J_7(i,i)=(1+\frac{\Delta t}{2T_{Ai}}) \tag{3.102}$$

$$J_{10}:(\text{m x n}):\ \frac{\partial f_7}{\partial V}\quad :J_{10}(i,i)=\frac{\Delta t}{2T_{Ai}}K_{Ai} \tag{3.103}$$

$\Delta f_8 \leftrightarrow E_d^{'}, \delta, I_q, V, \theta$:

$$J_2 : (\text{m x m}): \frac{\partial f_8}{\partial E_d^{'}} \quad : J_2(i,i) = -1 \tag{3.104}$$

$$J_3 : (\text{m x m}): \frac{\partial f_8}{\partial \delta} \quad : J_3(i,i) = V_i \cos(\delta_i - \theta_i) \tag{3.105}$$

$$J_9 : (\text{m x m}): \frac{\partial f_8}{\partial I_q} \quad : J_9(i,i) = -X_{qi}^{'} \tag{3.106}$$

$$J_{10} : (\text{m x n}): \frac{\partial f_8}{\partial V} \quad : J_{10}(i,i) = \sin(\delta_i - \delta_i) \tag{3.107}$$

$$J_{11} : (\text{m x n}): \frac{\partial f_8}{\partial \theta} \quad : J_{11}(i,i) = -V_i \cos(\delta_i - \delta_i) \tag{3.108}$$

$\Delta f_9 \leftrightarrow E_q^{'}, \delta, I_d, V, \theta$:

$$J_1 : (\text{m x m}): \frac{\partial f_9}{\partial E_q^{'}} \quad : J_1(i,i) = -1 \tag{3.109}$$

$$J_3 : (\text{m x m}): \frac{\partial f_9}{\partial \delta} \quad : J_3(i,i) = -V_i \sin(\delta_i - \theta_i) \tag{3.110}$$

$$J_8 : (\text{m x m}): \frac{\partial f_9}{\partial I_d} \quad : J_8(i,i) = X_{di}^{'} \tag{3.111}$$

$$J_{10} : (\text{m x n}): \frac{\partial f_9}{\partial V} \quad : J_{10}(i,i) = \cos(\delta_i - \delta_i) \tag{3.112}$$

$$J_{11} : (\text{m x n}): \frac{\partial f_9}{\partial \theta} \quad : J_{11}(i,i) = V_i \sin(\delta_i - \delta_i) \tag{3.113}$$

Part 2: DFIG

$\Delta g_1 \leftrightarrow i_{ds}, i_{qs}, e_d, V, \theta$

$$J_1 : (\text{g x g}): \frac{\partial g_1}{\partial i_{ds}} \quad : J_1(i,i) = R_{si} \tag{3.114}$$

$$J_2 : (\text{g x g}): \frac{\partial g_1}{\partial i_{qs}} \quad : J_2(i,i) = X_i^{'} \tag{3.115}$$

$$J_3 : (\text{g x g}): \frac{\partial g_1}{\partial e_d} \quad : J_3(i,i) = 1 \tag{3.116}$$

$$J_{13} : (\text{g x g}): \frac{\partial g_1}{\partial V} \quad : J_{13}(i,i) = -\cos(\theta_i) \tag{3.117}$$

$$J_{14}:(\text{g x g}):\ \frac{\partial g_1}{\partial \theta} \quad : J_{14}(i,i) = V_i \sin(\theta_i) \tag{3.118}$$

$\Delta g_2 \leftrightarrow i_{ds}, i_{qs}, e_q, V, \theta$

$$J_1:(\text{g x g}):\ \frac{\partial g_2}{\partial i_{ds}} \quad : J_1(i,i) = -X_i' \tag{3.119}$$

$$J_2:(\text{g x g}):\ \frac{\partial h_2}{\partial i_{qs}} \quad : J_2(i,i) = -R_{si} \tag{3.120}$$

$$J_4:(\text{g x g}):\ \frac{\partial g_2}{\partial e_q} \quad : J_4(i,i) = 1 \tag{3.121}$$

$$J_{13}:(\text{g x g}):\ \frac{\partial g_2}{\partial V} \quad : J_{13}(i,i) = -\sin(\theta_i) \tag{3.122}$$

$$J_{14}:(\text{g x g}):\ \frac{\partial g_2}{\partial \theta} \quad : J_{14}(i,i) = -V_i \cos(\theta_i) \tag{3.123}$$

$\Delta g_3 \leftrightarrow i_{qs}, e_d, e_q, \omega_r, v_{qr}$

$$J_2:(\text{g x g}):\ \frac{\partial g_3}{\partial i_{qs}} \quad : J_2(i,i) = -\frac{\Delta t}{2T_{oi}}(X_i - X_i') \tag{3.124}$$

$$J_3:(\text{g x g}):\ \frac{\partial g_3}{\partial e_d} \quad : J_3(i,i) = \left(1 + \frac{\Delta t}{2T_{oi}}\right) \tag{3.125}$$

$$J_4:(\text{g x g}):\ \frac{\partial g_3}{\partial e_q} \quad : J_4(i,i) = -\frac{\Delta t}{2} s_i \omega_{si} \tag{3.126}$$

$$J_5:(\text{g x g}):\ \frac{\partial g_3}{\partial \omega_r} \quad : J_5(i,i) = \frac{\Delta t}{2} e_{qi} \tag{3.127}$$

$$J_7:(\text{g x g}):\ \frac{\partial g_3}{\partial v_{qr}} \quad : J_7(i,i) = \frac{\Delta t}{2} \omega_{si} \frac{L_{mi}}{L_{rri}} \tag{3.128}$$

$\Delta g_4 \leftrightarrow i_{ds}, e_d, e_q, \omega_r, v_{dr}$

$$J_1:(\text{g x g}):\ \frac{\partial g_4}{\partial i_{ds}} \quad : J_1(i,i) = \frac{\Delta t}{2T_{oi}}(X_i - X_i') \tag{3.129}$$

$$J_3:(\text{g x g}):\ \frac{\partial g_4}{\partial e_d} \quad : J_3(i,i) = \frac{\Delta t}{2} s_i \omega_{si} \tag{3.130}$$

$$J_4:(\text{g x g}):\ \frac{\partial g_4}{\partial e_q} \quad : J_4(i,i) = \left(1 + \frac{\Delta t}{2T_{oi}}\right) \tag{3.131}$$

$$J_5:(\text{g x g}):\ \frac{\partial g_4}{\partial \omega_r} \quad : J_5(i,i) = -\frac{\Delta t}{2} e_{di} \tag{3.132}$$

$$J_6:(\text{g x g}):\ \frac{\partial g_4}{\partial v_{dr}} \quad : J_6(i,i) = -\frac{\Delta t}{2} \omega_{si} \frac{L_{mi}}{L_{rri}} \tag{3.133}$$

$\Delta g_5 \leftrightarrow i_{qs}, \omega_r, V$

$$J_2:(\text{g x g}):\ \frac{\partial g_5}{\partial i_{qs}} \quad : J_2(i,i) = -\frac{\Delta t}{2H_{ti}} \frac{V_i}{\omega_{si}} \tag{3.134}$$

$$J_5:(\text{g x g}):\ \frac{\partial g_5}{\partial \omega_r} \quad : J_5(i,i) = 1 \tag{3.135}$$

$$J_{13}:(\text{g x g}):\ \frac{\partial g_5}{\partial V} \quad : J_{13}(i,i) = -\frac{\Delta t}{4H_{ti}} \frac{i_{qsi}}{\omega_{si}} \tag{3.136}$$

$\Delta g_6 \leftrightarrow i_{ds}, \omega_r, v_{dr}, v'_{dr}, V$

$$J_1:(\text{g x g}):\ \frac{\partial g_6}{\partial i_{ds}} \quad : J_2(i,i) = -(\omega_{si} - \omega_{ri}) X_{2i} \frac{L_{ssi}}{L_{mi}} \tag{3.137}$$

$$J_5:(\text{g x g}):\ \frac{\partial g_6}{\partial \omega_r} \quad : J_5(i,i) = -X_{2i}\left(\frac{V_i}{\omega_{si} L_{mi}} - \frac{L_{ssi}}{L_{mi}} i_{dsi}\right) \tag{3.138}$$

$$J_6:(\text{g x g}):\ \frac{\partial g_6}{\partial v_{dr}} \quad : J_6(i,i) = 1 \tag{3.139}$$

$$J_7:(\text{g x g}):\ \frac{\partial h_6}{\partial v'_{dr}} \quad : J_6(i,i) = -1 \tag{3.140}$$

$$J_{13}:(\text{g x g}):\ \frac{\partial g_6}{\partial V} \quad : J_{13}(i,i) = (\omega_{si} - \omega_{ri}) X_{2i} \frac{1}{\omega_{si} L_{mi}} \tag{3.141}$$

$\Delta g_7 \leftrightarrow i_{dr\,ref}, V$

$$J_8:(\text{g x g}):\ \frac{\partial g_7}{\partial e_{dr\,ref}} \quad : J_8(i,i) = \left(1 + \frac{\Delta t}{2} K_{I3i}\right) \tag{3.142}$$

$$J_{13}:(\text{g x g}):\ \frac{\partial g_7}{\partial V} \quad : J_{13}(i,i) = -\frac{\Delta t}{2} K_{I3i}\left(K_{P3i} - \frac{1}{\omega_{si} L_{mi}}\right) \tag{3.143}$$

$\Delta g_8 \leftrightarrow i_{ds}, i_{dr\,ref}, v'_{dr}, V$

$$J_1:(\text{g x g}):\ \frac{\partial g_8}{\partial i_{ds}} \quad : J_1(i,i) = -\left(K_{P2i} + \frac{\Delta t}{2} K_{I2i}\right) \frac{L_{ssi}}{L_{mi}} \tag{3.144}$$

$$J_8:(\mathrm{g\ x\ g}):\ \frac{\partial g_8}{\partial i_{dr\,ref}}\quad :J_8(i,i)=\left(K_{P2i}+\frac{\Delta t}{2}K_{I2i}\right) \tag{3.145}$$

$$J_9:(\mathrm{g\ x\ g}):\ \frac{\partial g_8}{\partial v'_{dr}}\quad :J_9(i,i)=1 \tag{3.146}$$

$$J_{13}:(\mathrm{g\ x\ g}):\ \frac{\partial g_8}{\partial V}\quad :J_{13}(i,i)=\left(K_{P2i}+\frac{\Delta t}{2}K_{I2i}\right)\frac{1}{\omega_{si}L_{mi}} \tag{3.147}$$

$\Delta g_9 \leftrightarrow i_{ds}, \omega_r, v_{qr}, v'_{qr}, V$

$$J_1:(\mathrm{g\ x\ g}):\ \frac{\partial g_9}{\partial i_{ds}}\quad :J_2(i,i)=(\omega_{si}-\omega_{ri})X_{2i}\frac{L_{ssi}}{L_{mi}} \tag{3.148}$$

$$J_5:(\mathrm{g\ x\ g}):\ \frac{\partial g_9}{\partial \omega_r}\quad :J_5(i,i)=\left[X_{2i}\left(\frac{V_i}{\omega_{si}L_{mi}}-\frac{L_{ssi}}{L_{mi}}i_{dsi}\right)+\frac{L_{mi}}{L_{ssi}}\frac{V_i}{\omega_{si}}\right] \tag{3.149}$$

$$J_7:(\mathrm{g\ x\ g}):\ \frac{\partial g_9}{\partial v_{qr}}\quad :J_7(i,i)=1 \tag{3.150}$$

$$J_{10}:(\mathrm{g\ x\ g}):\ \frac{\partial g_9}{\partial v'_{qr}}\quad :J_{10}(i,i)=-1 \tag{3.151}$$

$$J_{13}:(\mathrm{g\ x\ g}):\ \frac{\partial g_9}{\partial V}\quad :J_{13}(i,i)=-(\omega_{si}-\omega_{ri})\left[\frac{X_{2i}}{\omega_{si}L_{mi}}+\frac{L_{mi}}{\omega_{si}L_{ssi}}\right] \tag{3.152}$$

$\Delta g_{10} \leftrightarrow i_{qs}, \omega_r, v'_{qr}, V$

$$J_2:(\mathrm{g\ x\ g}):\ \frac{\partial g_{10}}{\partial i_{qs}}\quad :J_2(i,i)=\left(K_{P2i}+\frac{\Delta t}{2}K_{I2i}\right)\frac{L_{ssi}}{L_{mi}} \tag{3.153}$$

$$J_5:(\mathrm{g\ x\ g}):\ \frac{\partial g_{10}}{\partial \omega_r}\quad :J_5(i,i)=2\left(K_{P2i}+\frac{\Delta t}{2}K_{I2i}\right)K_{opti}\frac{L_{ssi}}{L_{mi}}\frac{\omega_{ri}}{V_i} \tag{3.154}$$

$$J_{10}:(\mathrm{g\ x\ g}):\ \frac{\partial g_{10}}{\partial v'_{vqr}}\quad :J_{10}(i,i)=1 \tag{3.156}$$

$$J_{13}:(\mathrm{g\ x\ g}):\ \frac{\partial g_{10}}{\partial V}\quad :J_{13}(i,i)=-\left(K_{P2i}+\frac{\Delta t}{2}K_{I2i}\right)K_{opti}\frac{L_{ssi}}{L_{mi}}\left(\frac{\omega_{ri}}{V_i}\right)^2 \tag{3.157}$$

Part 3: For Network equations

For Infinite bus and synchronous machine buses:

$\Delta h_1 \leftrightarrow \delta, I_d, I_q, V, \theta$:

$$J_1 : (\text{m x m}): \frac{\partial h_1}{\partial \delta} \quad : J_1(i,i) = -I_{di} V_i \cos(\delta_i - \theta_i) + I_{qi} V_i \sin(\delta_i - \theta_i) \tag{3.158}$$

$$J_2 : (\text{m x m}): \frac{\partial h_1}{\partial I_d} \quad : J_2(i,i) = -V_i \sin(\delta_i - \theta_i) \tag{3.159}$$

$$J_3 : (\text{m x m}): \frac{\partial h_1}{\partial I_q} \quad : J_3(i,i) = -V_i \cos(\delta_i - \theta_i) \tag{3.160}$$

$$J_4 : (\text{m x n}): \frac{\partial h_1}{\partial V} \quad : J_4(i,i) = 2V_i G_{ii} - I_{di} \sin(\delta_i - \theta_i) - I_{qi} \cos(\delta_i - \theta_i) + \sum_{\substack{k=1 \\ k \neq i}}^{n} V_k Y_{ik} \cos(\theta_i - \theta_k - \alpha_{ik}) \tag{3.161}$$

$$J_4(i,k) = V_i Y_{ik} \cos(\theta_i - \theta_k - \alpha_{ik}) \tag{3.162}$$

$$J_5 : (\text{m x n}): \frac{\partial h_1}{\partial \theta} \quad : J_5(i,i) = +V_i I_{di} \cos(\delta_i - \theta_i) - V_i I_{qi} \sin(\delta_i - \theta_i) - \sum_{\substack{k=1 \\ k \neq i}}^{n} V_i V_k Y_{ik} \sin(\theta_i - \theta_k - \alpha_{ik}) \tag{3.163}$$

$$J_5(i,k) = V_i V_k Y_{ik} \sin(\theta_i - \theta_k - \alpha_{ik}) \tag{3.164}$$

$\Delta h_2 \leftrightarrow \delta, I_d, I_q, V, \theta$:

$$J_1 : (\text{m x m}): \frac{\partial h_2}{\partial \delta} \quad : J_1(i,i) = I_{di} V_i \sin(\delta_i - \theta_i) + I_{qi} V_i \cos(\delta_i - \theta_i) \tag{3.165}$$

$$J_2 : (\text{m x m}): \frac{\partial h_2}{\partial I_d} \quad : J_2(i,i) = -V_i \cos(\delta_i - \theta_i) \tag{3.166}$$

$$J_3 : (\text{m x m}): \frac{\partial h_2}{\partial I_q} \quad : J_3(i,i) = V_i \sin(\delta_i - \theta_i) \tag{3.167}$$

$$J_4 : (\text{m x n}): \frac{\partial h_2}{\partial V} \quad : J_4(i,i) = -2V_i B_{ii} - I_{di} \cos(\delta_i - \theta_i) + I_{qi} \sin(\delta_i - \theta_i) + \sum_{\substack{k=1 \\ k \neq i}}^{n} V_k Y_{ik} \sin(\theta_i - \theta_k - \alpha_{ik}) \tag{3.168}$$

$$J_4(i,k) = V_i Y_{ik} \sin(\theta_i - \theta_k - \alpha_{ik}) \tag{3.169}$$

$$J_5:(\text{m x n}):\ \frac{\partial h_2}{\partial \theta} \quad : J_5(i,i) = -V_i I_{di}\sin(\delta_i-\theta_i) - V_i I_{qi}\cos(\delta_i-\theta_i) + \sum_{\substack{k=1\\k\neq i}}^{n} V_i V_k Y_{ik}\cos(\theta_i-\theta_k-\alpha_{ik}) \tag{3.170}$$

$$J_5(i,k) = -V_i V_k Y_{ik}\cos(\theta_i-\theta_k-\alpha_{ik}) \tag{3.171}$$

For DFIG buses:

$\Delta h_3 \leftrightarrow i_{ds}, i_{qs}, v_{dr}, v_{qr}, V, \theta$:

$$J_1:(\text{g x g}):\ \frac{\partial h_3}{\partial i_{ds}} \quad : J_1(i,i) = V_i\cos(\theta_i) + \frac{L_{ssi}}{L_{mi}} v_{dri} \tag{3.172}$$

$$J_2:(\text{g x g}):\ \frac{\partial h_3}{\partial i_{qs}} \quad : J_2(i,i) = V_i\sin(\theta_i) - \frac{L_{ssi}}{L_{mi}} v_{qri} \tag{3.173}$$

$$J_6:(\text{g x g}):\ \frac{\partial h_3}{\partial v_{dr}} \quad : J_6(i,i) = -\left[\frac{V_i}{\omega_{si} L_{mi}} - \frac{L_{ssi}}{L_{mi}} i_{dsi}\right] \tag{3.174}$$

$$J_7:(\text{g x g}):\ \frac{\partial h_3}{\partial v_{qr}} \quad : J_7(i,i) = -\frac{L_{ssi}}{L_{mi}} i_{qsi} \tag{3.175}$$

$$J_{13}:(\text{g x g}):\ \frac{\partial h_3}{\partial V} \quad : J_{13}(i,i) = i_{dsi}\cos(\theta_i) + i_{qsi}\sin(\theta_i) - \frac{v_{dri}}{\omega_{si} L_{mi}} - 2V_i Y_{ii}\cos(\alpha_{ii})... - \sum_{\substack{k=1\\k\neq i}}^{n} V_k Y_{ik}\cos(\theta_i-\theta_k-\alpha_{ik}) \tag{3.176}$$

$$J_{13}(i,k) = -V_i Y_{ik}\cos(\theta_i-\theta_k-\alpha_{ik}) \tag{3.177}$$

$$J_{14}:(\text{g x g}):\ \frac{\partial h_3}{\partial \theta} \quad : J_{14}(i,i) = -V_i i_{dsi}\sin(\theta_i) + V_i i_{qsi}\cos(\theta_i) + \sum_{\substack{k=1\\k\neq i}}^{n} V_i V_k Y_{ik}\sin(\theta_i-\theta_k-\alpha_{ik}) \tag{3.178}$$

$$J_{14}(i,k) = -V_i V_k Y_{ik}\sin(\theta_i-\theta_k-\alpha_{ik}) \tag{3.179}$$

$\Delta h_4 \leftrightarrow i_{ds}, V, \theta$:

$$J_1:(\text{g x g}):\ \frac{\partial h_4}{\partial i_{ds}} \quad : J_1(i,i) = -V_i \tag{3.179}$$

$$J_{13}:(\text{g x g}):\ \frac{\partial h_4}{\partial V} \quad : J_{13}(i,i) = -i_{dsi} + 2V_i Y_{ii}\sin(\alpha_{ii}) - \sum_{\substack{k=1\\k\neq i}}^{n} V_k Y_{ik}\sin(\theta_i-\theta_k-\alpha_{ik}) \tag{3.180}$$

$$J_{13}(i,k) = -V_i Y_{ik}\sin(\theta_i-\theta_k-\alpha_{ik}) \tag{3.181}$$

$$J_{14}:(\text{g x g}):\ \frac{\partial h_4}{\partial \theta} \quad : J_{14}(i,i) = -\sum_{\substack{k=1 \\ k\neq i}}^{n} V_i V_k Y_{ik} \cos(\theta_i - \theta_k - \alpha_{ik}) \tag{3.182}$$

$$J_{14}(i,k) = +V_i V_k Y_{ik} \cos(\theta_i - \theta_k - \alpha_{ik}) \tag{3.183}$$

For load buses:

$\Delta h_5 \leftrightarrow V, \theta$:

$$J_1:((\text{n - m}) \text{ x n}):\ \frac{\partial h_5}{\partial V} \quad : J_1(i,i) = 2V_i G_{ii} + \sum_{\substack{k=1 \\ k\neq i}}^{n} V_k Y_{ik} \cos(\theta_i - \theta_k - \alpha_{ik}) \tag{3.184}$$

$$J_1(i,k) = V_i Y_{ik} \cos(\theta_i - \theta_k - \alpha_{ik}) \tag{3.185}$$

$$J_2:((\text{n - m}) \text{ x n}):\ \frac{\partial h_5}{\partial \theta} \quad : J_2(i,i) = -\sum_{\substack{k=1 \\ k\neq i}}^{n} V_i V_k Y_{ik} \sin(\theta_i - \theta_k - \alpha_{ik}) \tag{3.186}$$

$$J_2(i,k) = V_i V_k Y_{ik} \sin(\theta_i - \theta_k - \alpha_{ik}) \tag{3.187}$$

$\Delta h_6 \leftrightarrow V, \theta$:

$$J_1:((\text{n - m}) \text{ x n}):\ \frac{\partial h_6}{\partial V} \quad : J_1(i,i) = -2V_i B_{ii} + \sum_{\substack{k=1 \\ k\neq i}}^{n} V_k Y_{ik} \sin(\theta_i - \theta_k - \alpha_{ik}) \tag{3.188}$$

$$J_1(i,k) = V_i Y_{ik} \sin(\theta_i - \theta_k - \alpha_{ik}) \tag{3.189}$$

$$J_2:((\text{n - m})\text{x n}):\ \frac{\partial h_6}{\partial \theta} \quad : J_2(i,i) = \sum_{\substack{k=1 \\ k\neq i}}^{n} V_i V_k Y_{ik} \cos(\theta_i - \theta_k - \alpha_{ik}) \tag{3.190}$$

$$J_2(i,k) = -V_i V_k Y_{ik} \cos(\theta_i - \theta_k - \alpha_{ik}) \tag{3.191}$$

Thus the required equations for simulation are given above and are used in developing the software for transient stability analysis of grid connected DFIG. In the next chapter, simulation results of this dissertation work are presented.

Chapter 4

SIMULATION RESULTS on DFIG-Infinite Bus System

4.1 Introduction

In this chapter, simulation results on a 8 bus power system network [9], which include a DFIG and an infinite bus, are presented. Figure 4.1 shows the 8 bus power system network with a DFIG and an infinite bus.

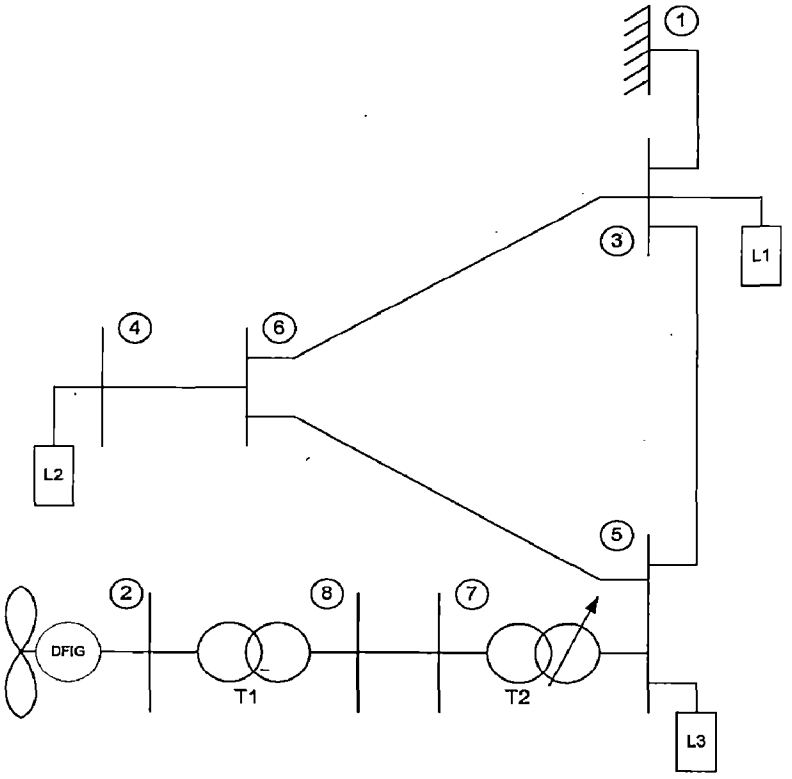

Figure 4.1: 8 bus power system network with a DFIG and an Infinite bus.

The network in Figure 4.1 consists of 8 buses, 3 loads, 2 transformers, a DFIG and an infinite bus. Bus 1 has been considered to be as an infinite bus. At bus 2 DFIG rated at 2 MW, 690V has been connected. Transformer T1 of leakage reactance 5.9% transforms 690V at bus 2 to 11kV at bus 8. Transform T2 with leakage reactance of 10% transforms 11kV at bus 7 to 33kV at bus 5. Throughout this dissertation work, the tap changer of transformer T2 has been maintained at tap position 1. Constant impedance loads, L1, L2 and L3, have been connected at bus 3, 4 and 5 respectively.

4.2 TSA Simulation

4.2.1 Initial conditions

Initial conditions for the DFIG and the rest of the system elements in Fig. 4.1 were obtained following the steps presented in sections 3.1.1 and 3.1.2. The line data, bus data and machine data are provided in Appendix A. The DFIG has been modelled as a PQ bus and the infinite bus has been modeled as slack bus. The various loads, being constant impedance loads, have been included into the Y-bus. The DFIG model has been initialized by applying mechanical torque $T_m = 0.8$ at the generator rotor. The rotor speed ω_r has been obtained from the torque-speed curve shown in Fig. 4.2 [10]. Eq. 4.1 represents optimal torque/power-speed curve which is shown in Fig. 4.1 as A-B curve.

$$T_m = K_{opt}\omega_r^2 \tag{4.1}$$

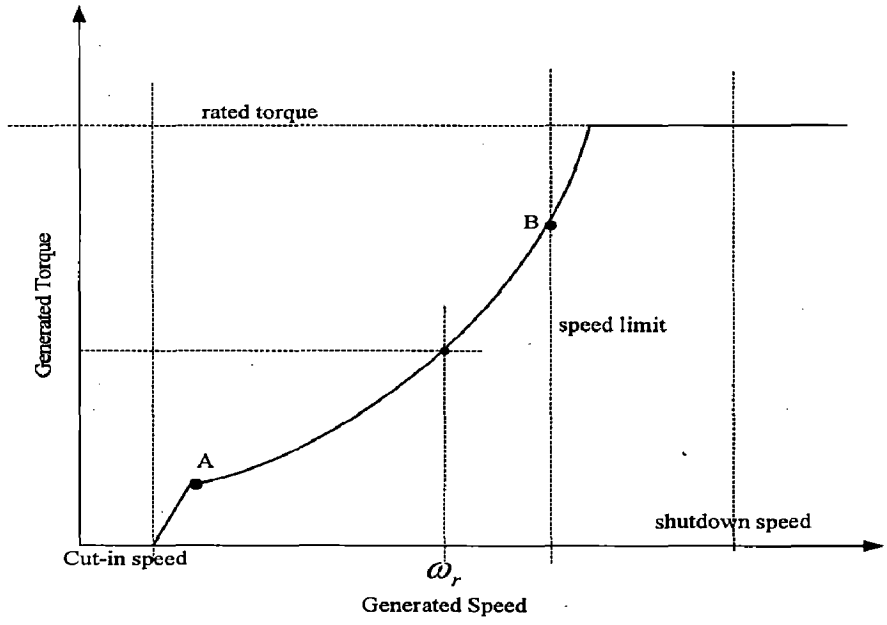

Figure 4.2: Torque-Speed characteristics for DFIG

Steady state values of generated active power P_g, generated active power Q_g and terminal voltage, obtained from the network load flow calculations, are used as the initial conditions. Table 4.1 shows the load flow results and Table 4.2 shows the initial conditions for various DFIG parameters. All the calculations and data are based on 100 MVA base.

Table 4.1: Load flow results for PQ representation of DFIG

Bus No.	Voltage (pu)	Angle (deg)	P_g (MW)	Q_g (MVAr)	P_L (MW)	Q_L (MVAr)
1	1.0000	0	4.47	2.08	0	0
2	0.9864	-0.1599	0.82	-0.96	0	0
3	0.9955	-0.4337	0	0	3.15	0.63
4	0.9885	-0.5975	0	0	1.20	0.24
5	0.9899	-0.4630	0	0	0.92	0.185
6	0.9900	-0.4993	0	0	0	0
7	0.9889	-0.4154	0	0	0	0
8	0.9870	-0.1882	0	0	0	0

Table 4.2: DFIG Initial conditions

i_{ds}	i_{qs}	e_d	e_q	ω_r
0.0098	-0.0162	1.1425	0.0857	1.1952
s	i_{dr}	i_{qr}	v_{dr}	v_{qr}
-0.1952	-0.0050	-0.0166	-0.2259	-0.0231

4.2.2 Fault Simulation results

The behaviour of the DFIG during fault was studied with a three phase fault at bus 4. The fault has been assumed to have taken place at t = 1.0s with clearing time of 100ms (fault cleared at 1.1s). For simulation, a time step of 0.001sec has been used. Simulation has been carried out for duration of 60s.

For optimizing the controller gains of Fig. 2.4 K_{P2}, K_{I2}, K_{P3} and K_{I3} PSO technique has been applied. This technique has been briefly explained in Appendix B. The objective was to minimize the normalized squared areas of the controller outputs, v_{dr} and v_{qr}, given by eqn. 4.2, by optimizing the controller gains. For a population size of 20 and iteration limit of 50, the objective has been achieved for 37 iterations and the optimized values obtained are $K_{P2} = 2.54102, K_{P3} = 0.0008, K_{I2} = 0.000065$ and $K_{I3} = 5.4539$.

$$\min(f) = \sum (v_{dr} - v_{dr\,ref})^2 + \sum (v_{qr} - v_{qr\,ref})^2 \qquad (4.2)$$

Where, $v_{dr\,ref}$ and $v_{qr\,ref}$ are the reference values of v_{dr} and v_{dr}

Figs. 4.3 - 4.8 show the behaviour of DFIG under fault condition. On application of fault on bus 4, current demanded becomes high which increases the DFIG stator current. This is accompanied with a reduction in the terminal voltage and

speed. And since i_{dr} and i_{qr} are directly proportional to the terminal voltage magnitude and stator q-axis current i_{qs} (3.16), we observe a decrease in their values. Once the fault is cleared, stator voltage is restored and demagnetized stator and rotor oppose this change. Fault clearing is also accompanied by increase in rotor speed. But because of the controller effect (2.15-2.19), which depends on the speed and rotor and stator currents, the system returns back to normal position in a few seconds.

In the next chapter, behaviour of DFIG for fault simulation has been observed when interconnected to a power system network containing synchronous machine. Also, simulation results of the synchronous machine without the interconnection of DFIG are presented.

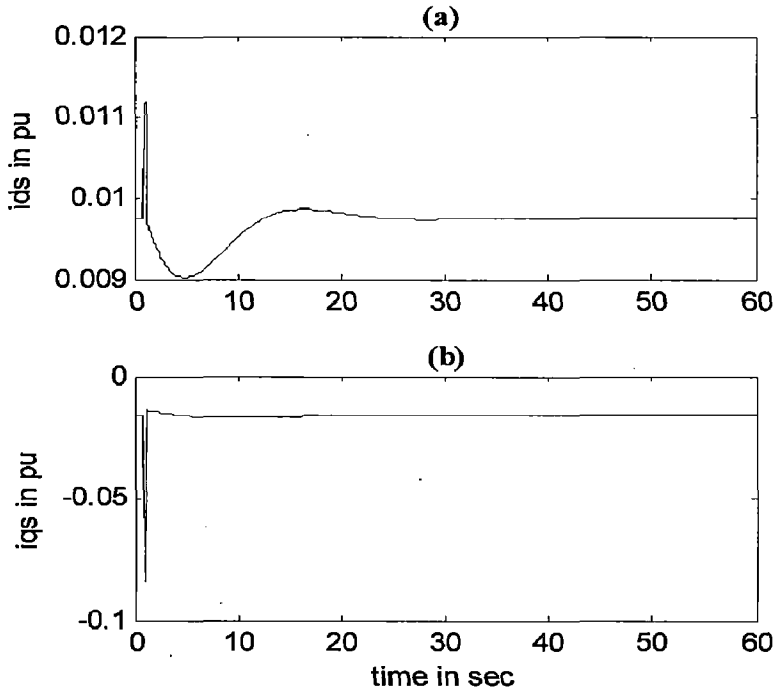

Figure 4.3: DFIG stator currents: (a) i_{ds} and (b) i_{qs}

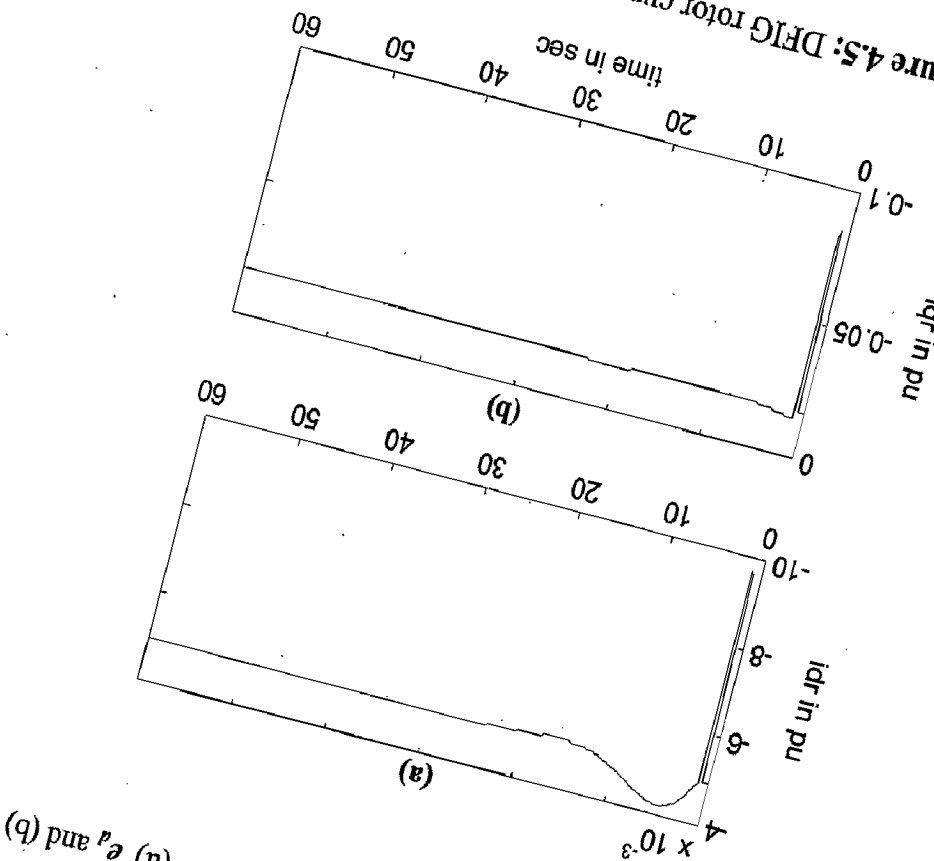

Figure 4.4: DFIG voltage behind transient reactance: (a) e_d and (b) e_q

Figure 4.5: DFIG rotor currents: (a) i_{dr} and (b) i_{qr}

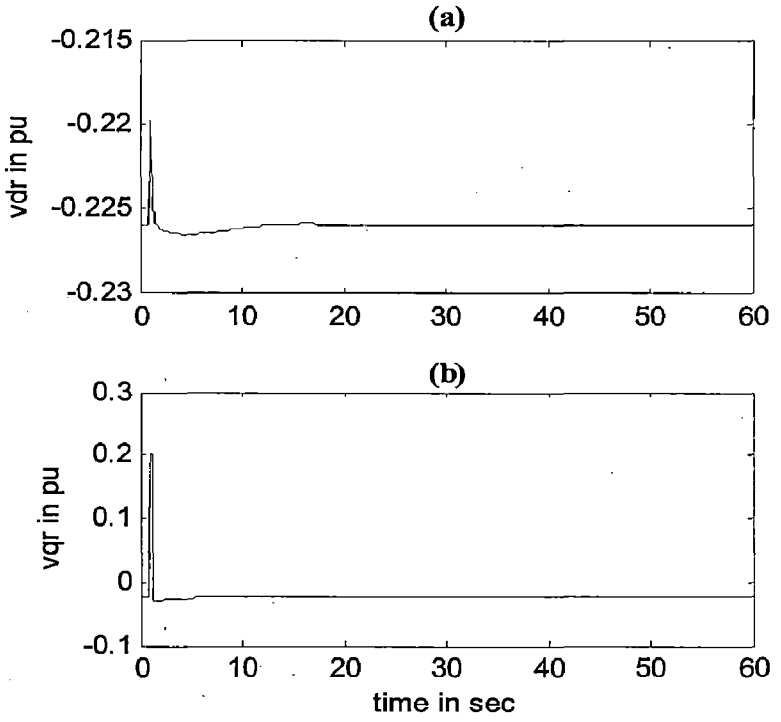

Figure 4.6: DFIG rotor voltages: (a) v_{dr} and (b) v_{qr}

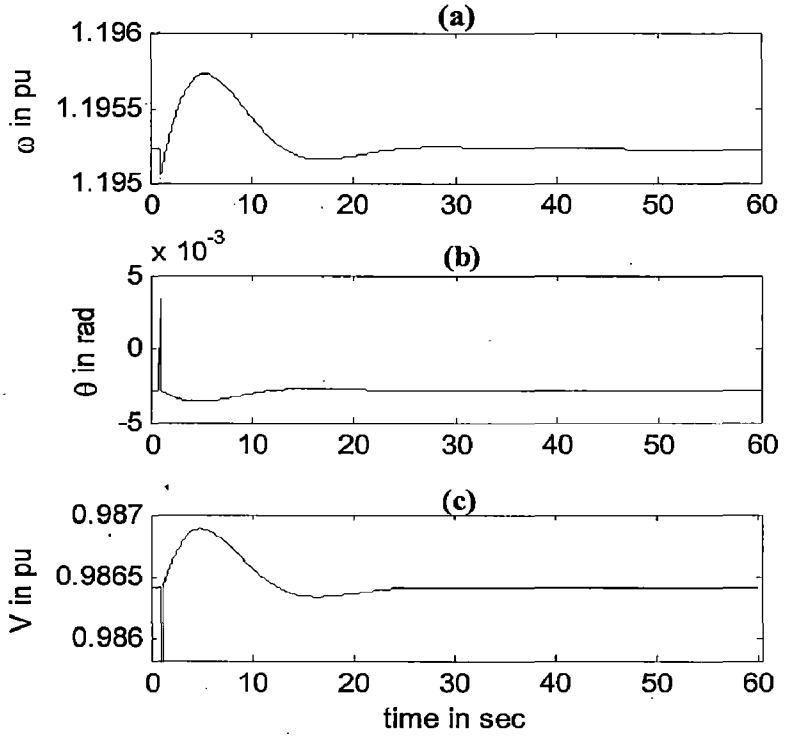

Figure 4.7: DIFG (a) rotor speed ω_r, (b) terminal voltage and (c) angle θ

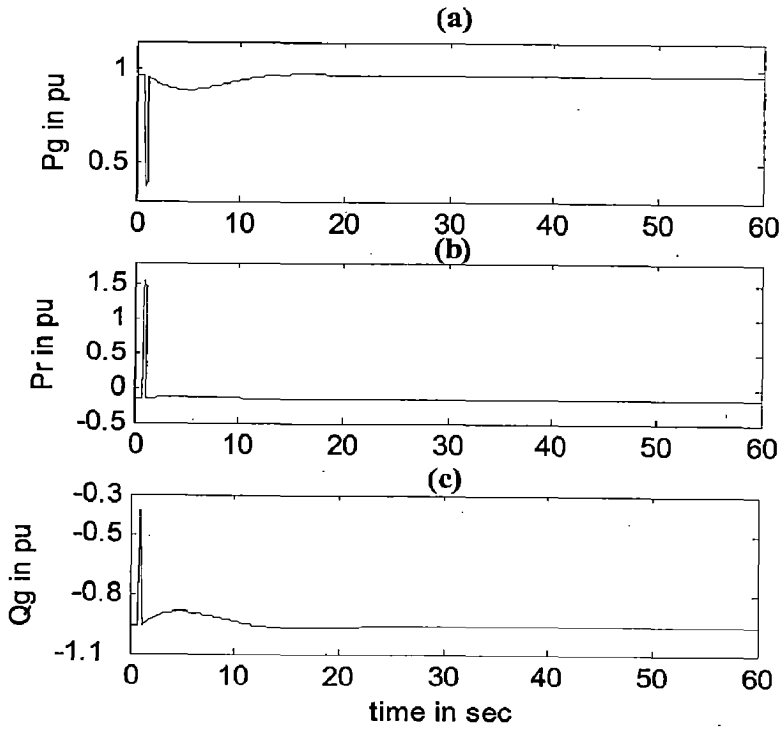

Figure 4.8: DFIG (a) generated real power P_g, (b) Rotor power P_r and (c) generated reactive power Q_g

Chapter 5

SIMULATION RESULTS on DFIG-Synchronous Machine System

5.1 Introduction

In this chapter, simulation studies have been carried out on a system containing both DFIG and synchronous machine (SM). Specifically, the 8 bus system as used in Chapter 4 has been used in this chapter also. To understand the dynamic interaction between the DFIG and SM properly, initially non-linear fault simulation studies have been carried out in the test system containing only the SM. Subsequently, simulation studies have been carried out on the test system containing both DFIG and SM. The two configurations of the test system considered in this chapter are shown in Figs. 5.1 and 5.2. The systems in Fig. 5.1 and Fig. 5.2 are modifications of Fig. 4.1 with a synchronous machine which has been connecting at bus 1. In Fig. 5.1 DFIG at bus 2 has been disconnected and consists only a synchronous machine at bus 1. Rest of the system descriptions remain unchanged and are as explained in section 4.1.

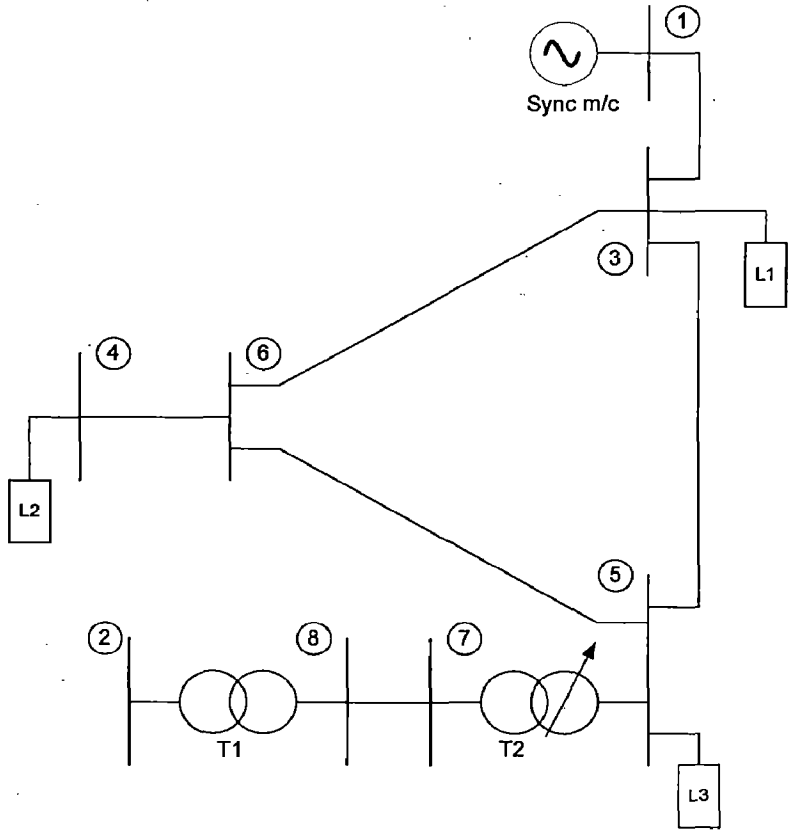

Figure 5.1: 8 bus power system network with a Synchronous machine.

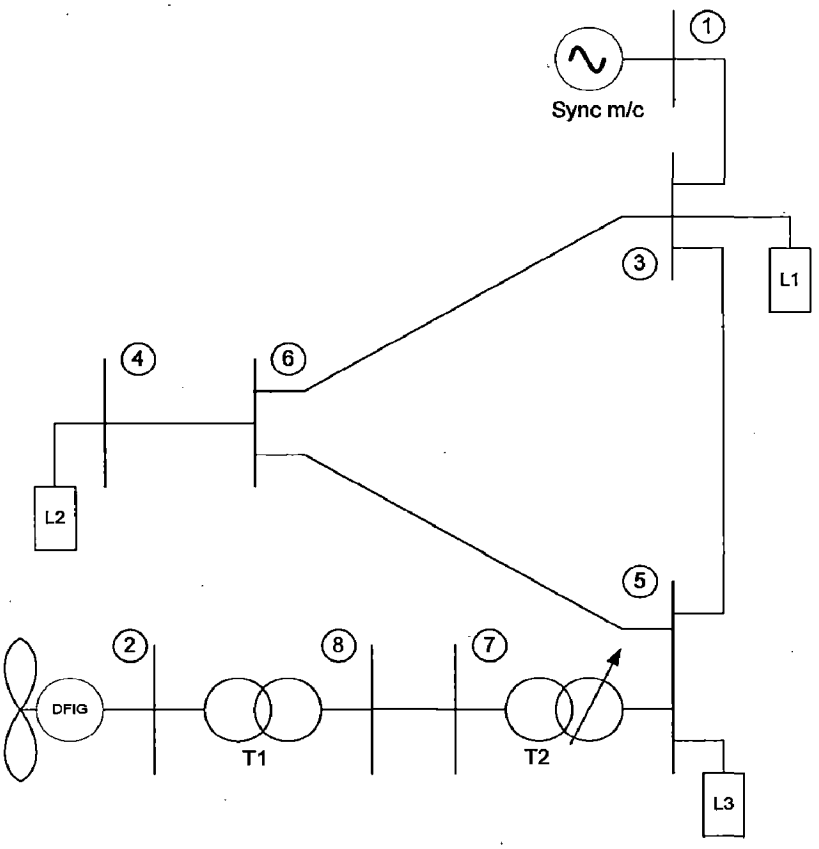

Figure 5.2: 8bus power system network with DFIG and Synchronous machine.

In the next sections, first initial conditions and TSA simulation results for synchronous machines are presented. Then the initial conditions and TSA simulation results for DFIG and synchronous machine together are presented.

5.2 TSA Simulation of 8 bus synchronous machine system

As described in the previous section, the system in Fig. 5.1 consists of a synchronous machine without interconnection of DFIG.

5.2.1 Initial conditions

Initial conditions for the system in Fig. 5.1 are obtained by following the procedures described in Sections 3.1.1 and 3.1.2. The line data, bus data and the machine data are provided in Appendix A. Table 5.1 shows the load flow results and Table 5.2 shows the initial conditions for the synchronous machine. All the calculations and data provided are based on 100MVA base.

Table 5.1: Load flow results for fault simulation of 8-bus synchronous machine system

Bus No.	Voltage (pu)	Angle (deg)	P_g (MW)	Q_g (MVAr)	P_L (MW)	Q_L (MVAr)
1	1	0	5.272	1.121	0	0
2	0.9969	-0.827	0	0	0	0
3	0.998	-0.535	0	0	3.151	0.631
4	0.9964	-0.933	0	0	1.2	0.24
5	0.9969	-0.827	0	0	0.92	0.185
6	0.9969	-0.825	0	0	0	0
7	0.9969	-0.827	0	0	0	0
8	0.9969	-0.827	0	0	0	0

Table 5.2: Initial conditions for Synchronous machine for fault simulation of 8-bus synchronous machine system

ω (rad/s)	I_d	I_q	V_d	V_q	V_{ref}
314.16	0.0115	0.0527	0.0051	1	1.051
E'_d	E'_q	E_{fd}	V_R	R_f	T_m
0	1.0007	1.0017	1.0202	0.1803	0.0527

5.2.2 Fault Simulation

A three phase fault has been applied on bus 4 at t = 1.0s and cleared at t = 1.1s. Using the SI-method described in section 3.2 simulation has been carried out for a period of 40s with a simulation step size of 0.001s. The simulation results for the synchronous machine are as shown in Figs. 5.3 to 5.5.

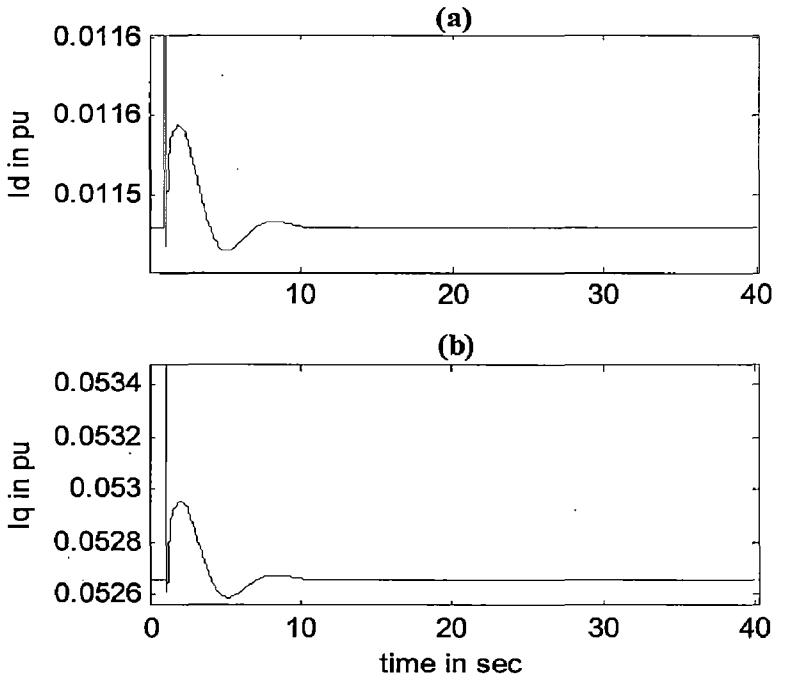

Figure 5.3: Synchronous machine stator currents for fault simulation of 8 bus synchronous machine system (a) I_d and (b) I_q

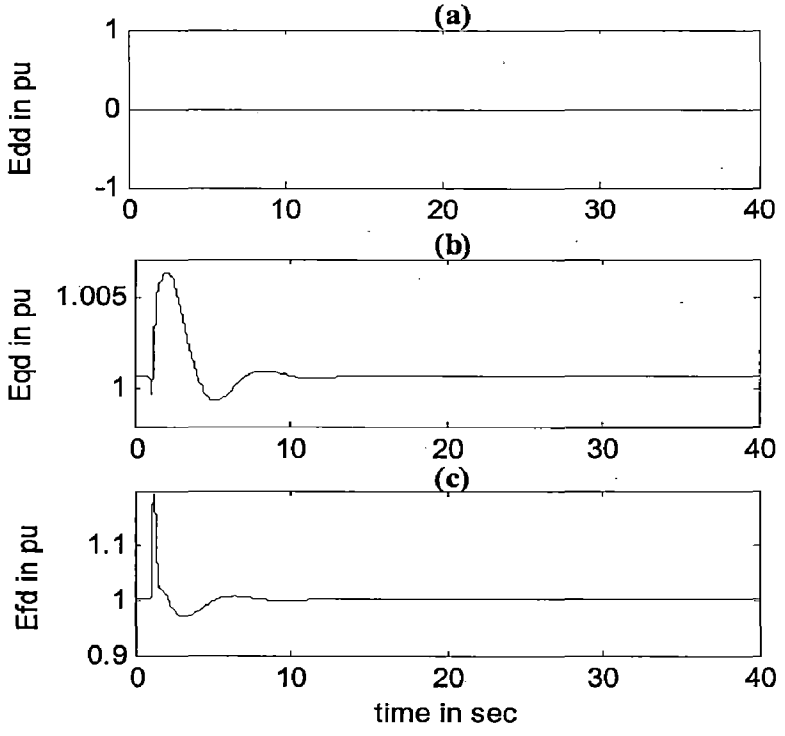

Figure 5.4: Synchronous machine (a) d-axis voltage behind transient reactance $E_d^{'}$ (b) q-axis voltage behind transient reactance $E_q^{'}$ and (c) Exciter output voltage E_{fd} for fault simulation of 8 bus synchronous machine system

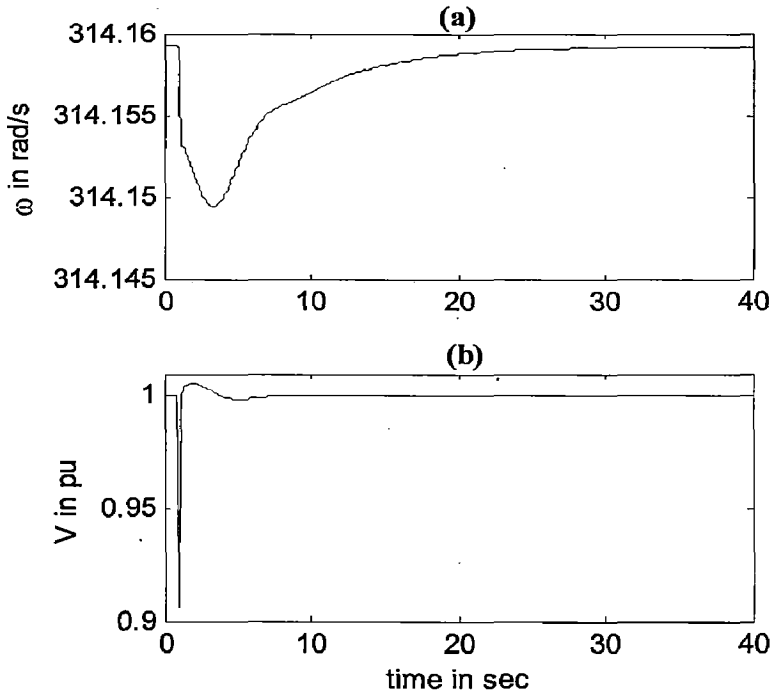

Figure 5.5: Synchronous machine (a) speed ω and (b) terminal voltage V for fault simulation of 8 bus synchronous machine system

5.3 TSA Simulation of 8 bus DFIG-Synchronous machine system

Fig. 5.2 shows the 8-bus system with a DFIG and a synchronous machine. In the previous section the behaviour of synchronous machine without the DFIG in the network has been presented. In this section a DFIG is connected at bus 2 and the behaviour of both the machines together in the system are presented.

5.3.1 Initial conditions

In this section initial conditions for DFIG and synchronous machine have been presented. First DFIG steady state values of generated active power P_g, generated active power Q_g and terminal voltage have been obtained from the network load flow calculations as explained in sections 3.1.1 and Fig 3.1 by modelling the DFIG as a PQ bus. DFIG and synchronous initial conditions have been obtained following the steps presented in section 3.1.2.

DFIG has been initialized for T_m=0.8 and ω_r has been calculated using (4.1). Table 5.3, 5.4 and 5.5 show the load flow results, DFIG initial conditions and synchronous machine initial conditions respectively.

Table 5.3: Load flow results for fault simulation of 8-bus DFIG-synchronous machine system

Bus No.	Voltage (pu)	Angle (deg)	P_g (MW)	Q_g (MVAr)	P_L (MW)	Q_L (MVAr)
1	1	0	4.47	2.08	0	0
2	0.9873	-0.2092	0.82	-0.96	0	0
3	0.9963	-0.4520	0	0	3.15	0.63
4	0.9925	-0.7558	0	0	1.20	0.24
5	0.9927	-0.6079	0	0	0.92	0.19
6	0.9930	-0.6470	0	0	0	0
7	0.9898	-0.4650	0	0	0	0
8	0.9879	-0.2375	0	0	0	0

Table 5.4: Initial conditions for DFIG for fault simulation of 8-bus DFIG-synchronous machine system

i_{ds}	i_{qs}	e_d	e_q	ω_r
0.0098	-0.0162	1.1433	0.085	1.1952
s	i_{dr}	i_{qr}	v_{dr}	v_{qr}
-0.1952	-0.0050	-0.0166	-0.2261	-0.0229

Table 5.5: Initial conditions for synchronous machine for fault simulation of 8-bus DFIG-synchronous machine system

ω	I_d	I_q	V_d	V_q	V_{ref}
314.16	0.021	0.0445	0.0043	1	1.051
E'_d	E'_q	E_{fd}	V_R	R_f	T_m
0	1.0013	1.0031	1.0217	0.1806	0.0446

5.3.2 Fault Simulation

A three fault has been simulated on bus 4, as explained in section 4.2.2, at time t=1.0s and subsequently the fault was cleared at t=1.1s. The simulation has been carried out for a period of 60s with a simulation step size of 0.001s. As the simulation time taken is considerably more, the DFIG controller gains K_{P2}, K_{I2}, K_{P3} and K_{I3} in this case have been obtained by trial and error method. The final values obtained are $K_{P2} = 2.1, K_{P3} = 0.007$, $K_{I2} = 0.0342$ and $K_{I3} = 5.4539$. The responses are shown in Figs. 5.6 – 5.13.

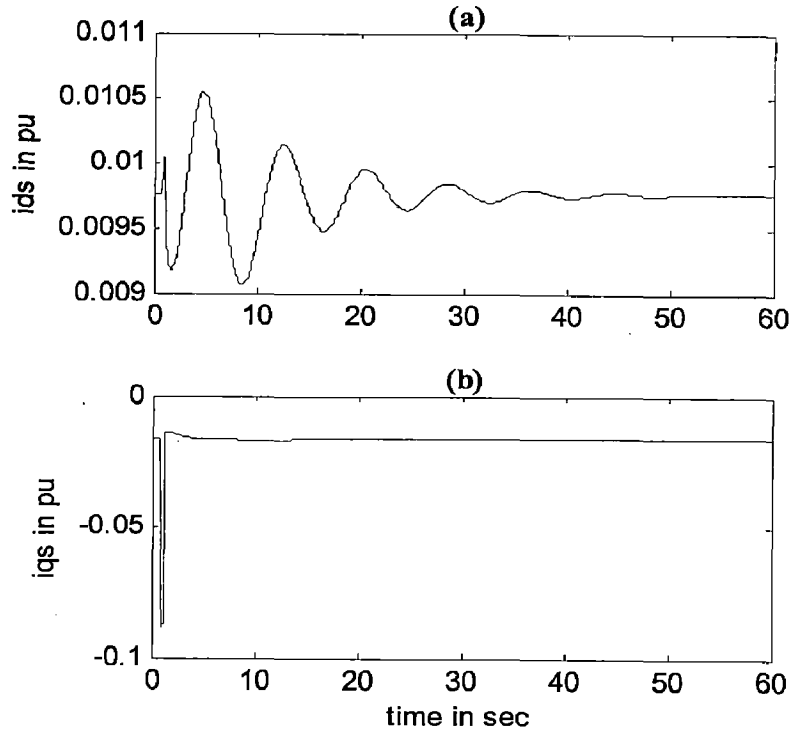

Figure 5.6: DFIG stator currents for fault simulation of 8 bus DFIG-synchronous machine system (a) i_{ds} and (b) i_{qs}

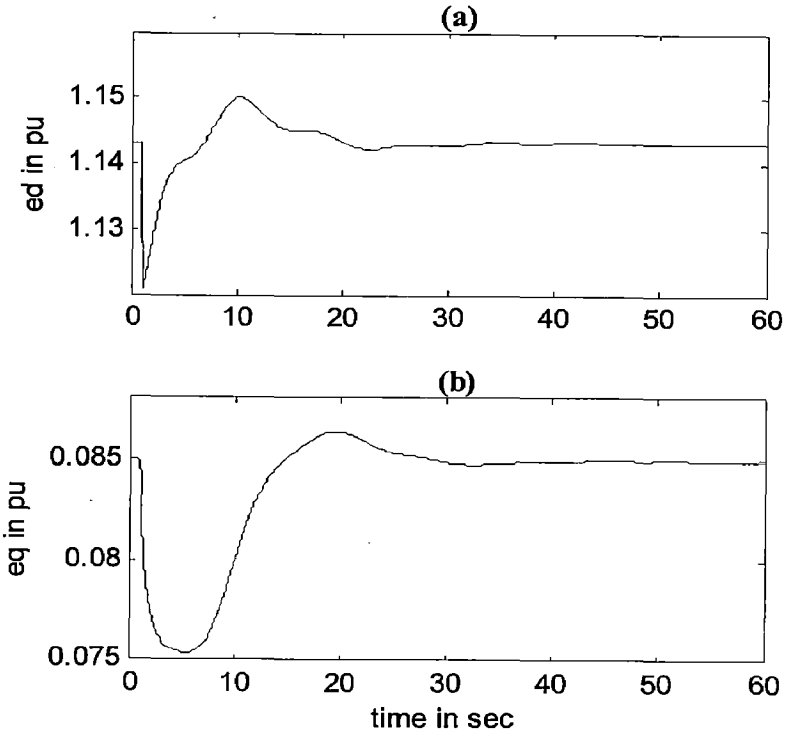

Figure 5.7: DFIG voltage behind transient reactance for fault simulation of 8 bus DFIG- synchronous machine system (a) e_d and (b) e_q

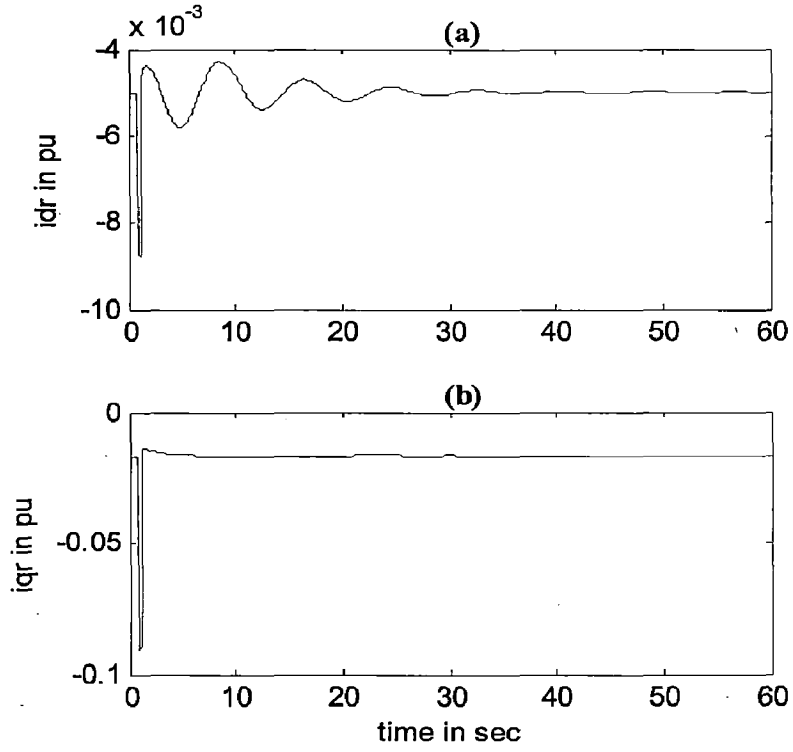

Figure 5.8: DFIG rotor currents for fault simulation of 8 bus DFIG-synchronous machine system (a) i_{dr} and (b) i_{qr}

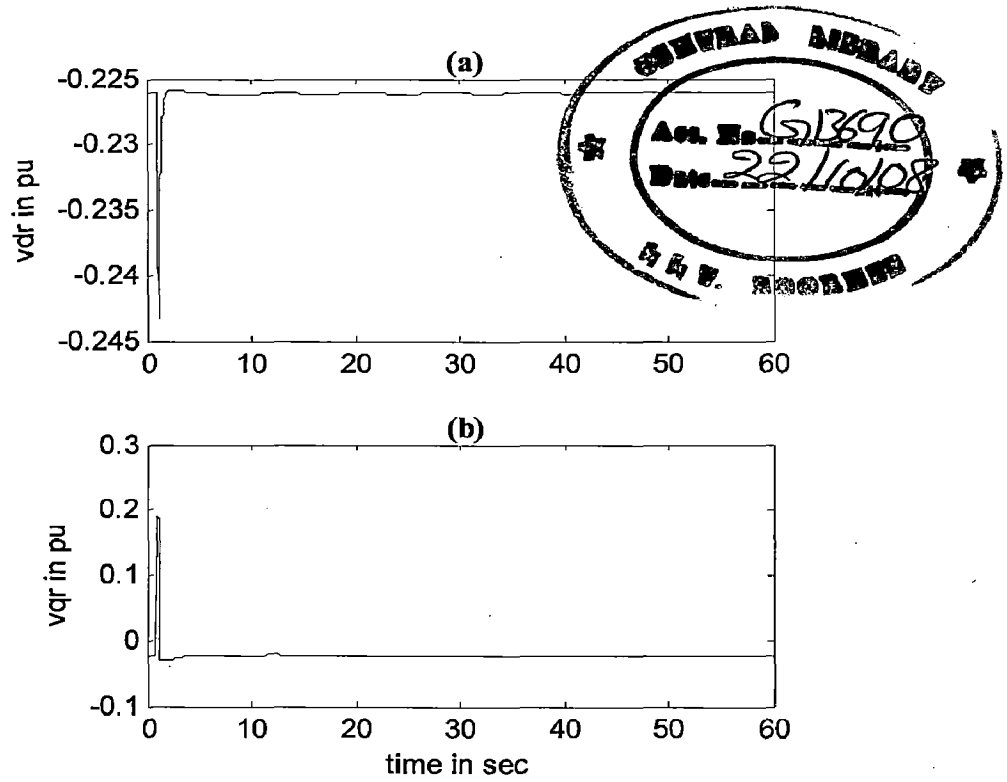

Figure 5.9: DFIG rotor voltages for fault simulation of 8 bus DFIG-synchronous machine system (a) v_{dr} and (b) v_{qr}

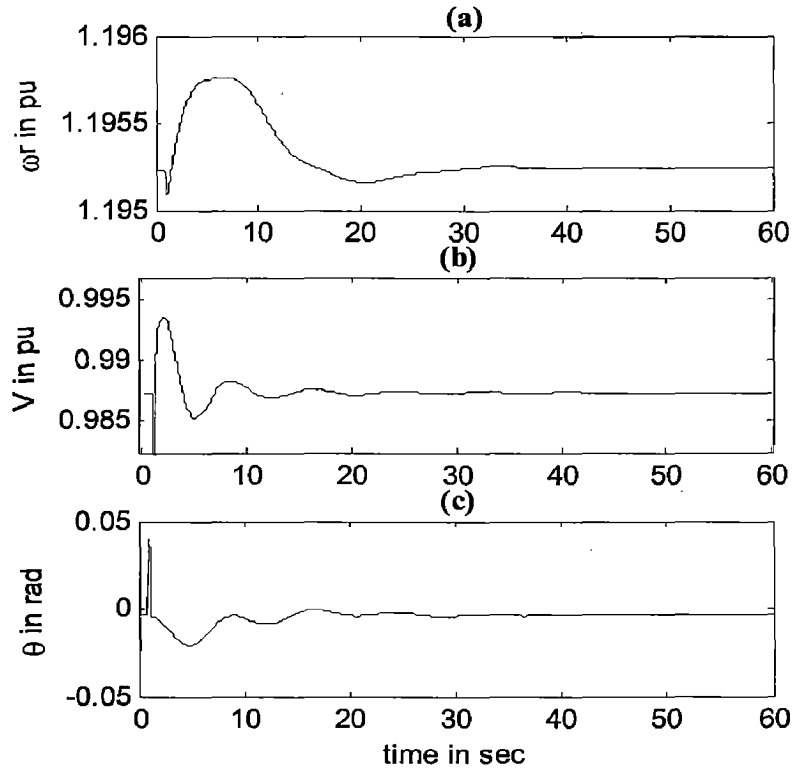

Figure 5.10: DIFG (a) rotor speed ω_r, (b) terminal voltage and (c) angle θ for fault simulation of 8 bus DFIG-synchronous machine system

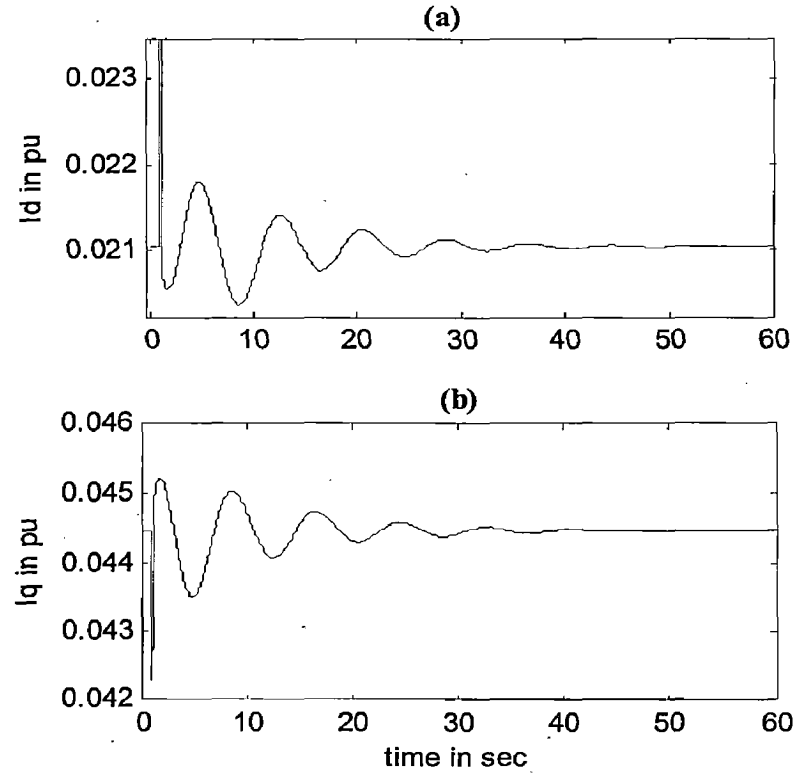

Figure 5.11: Synchronous machine stator currents for fault simulation of 8 bus DFIG- synchronous machine system (a) I_d and (b) I_q

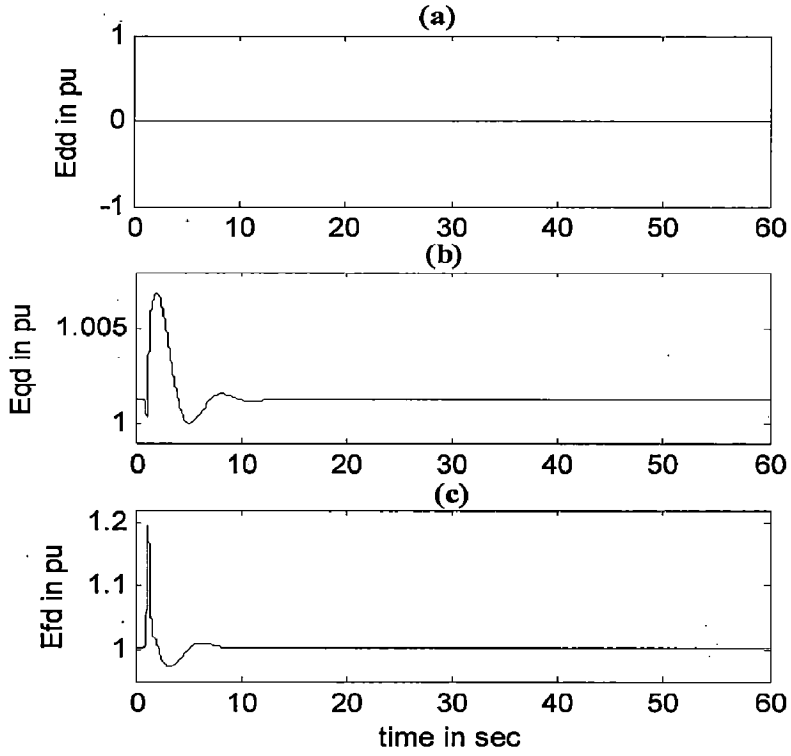

Figure 5.12: Synchronous machine (a) d-axis voltage behind transient reactance $E_d^{'}$, (b) q-axis voltage behind transient reactance $E_q^{'}$ and (c) Exciter output voltage E_{fd} for fault simulation of 8 bus DFIG-synchronous machine system

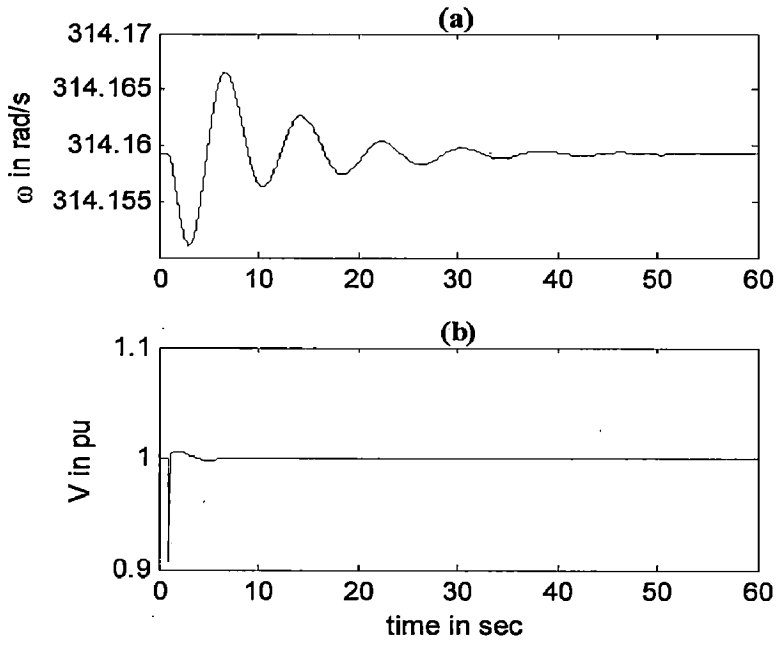

Figure 5.13: Synchronous machine (a) speed ω and (b) terminal voltage V for fault simulation of 8 bus DFIG- synchronous machine system

Comparing Fig. 5.13 and Fig. 5.5, it has been observed that, in the presence of the DFIG, the synchronous machine speed has become oscillatory and takes more time before settling to its steady state value, while there has been no considerable change in the voltage behaviour. Similar changes have been observed in synchronous machine stator currents I_d and I_d in Fig. 5.3 and Fig. 5.11 and rest of the parameters. Comparing Fig. 4.3 and Fig. 5.6, while there has been no considerable change in DFIG q-axis stator current behaviour, d-axis stator current becomes more oscillatory and there has been a delay in settling to its steady state value.

This comparison has shown that dynamic properties of DFIG have affected synchronous machine when both are present in the same power system network and vise versa. But, because of the controller actions of the DFIG, the DFIG and hence the system, remain stable under fault conditions.

Chapter 6
CONCLUSION

In this dissertation, the modelling and controller for DFIG has been described. Its performance under disturbances has been studied. A reduced order model has been used for ease of calculations and reduced simulation time. The main assumptions in the model used were neglect of stator transients and saturation effects. Modelling of synchronous machine and its performance with DFIG interconnection has also been studied. A 7^{th} order synchronous machine model has been used.

The models were implemented using SI-method, a numerical method widely used in industries now-a-days. Simulation studies have been carried out using MATLAB R2006a and PSO has been used to optimize the DFIG controller gains.

A 8-bus system has been used to study the effect of three phase faults on the stability of the system with three different combinations of DFIG and synchronous machine.

From the results shown in sections 4.2.2, 5.2.2 and 5.3.2, it has been observed that, the behaviour of both DFIG and synchronous machine under fault conditions has been affected by each other's presence in the power system network. When connected to infinite bus system (Fig. 4.1, which is a strong network) and to a synchronous machine system (Fig. 5.2, which is a weaker network), the DFIG remains stable for both the cases. This shows that DFIG is capable of withstanding grid faults when interconnected with the grid. This is one of the major advantages of DFIG when compared to its other equivalent machine types. Also, DFIG-based wind generation with the basic control scheme used provides better performance in terms of voltage control and damping.

In this dissertation, DFIG been modelled as a reduced order model, a compromise in accuracy has been done. In order to improve the accuracy of analysis and study, higher order models can be used. Also simulation time taken is considerably more. Better programming tools can be used to reduce the simulation time taken. An 8-bus system with only a DFIG and a Synchronous machine, which is comparatively a small network, has been used. But practical networks are much larger and complex. This dissertation can further be extended for larger, more practical

networks with interconnection of wind farms into the power system network. Also, there is a scope for improved speed controller and hence the performance of DFIG-based wind farms.

APPENDIX-A

8 BUS POWER SYSTEM DATA

A.1: Line Data - 8 Bus System [9] on 100MVA base

Table A.1: Line Data for 8 Bus System

From Bus	To Bus	Resistance (pu)	Reactance (pu)	Susceptance (pu)	Tap
1	3	0.01869	0.17726	0	1
3	6	0.31	0.40174	0	1
3	5	0.3329	0.5831	0	1
6	4	0.09	0.1577	0	1
6	5	0.06446	0.086	0	1
7	8	0.139	0.3104	0	1
5	7	0	0.1	0	1
8	2	0	0.059	0	1

A.2: Bus Data - 8 Bus System [9]

Table A.2: Bus Data for 8 Bus System

Bus No.	Bus Type	Voltage (pu)	Angle (deg)	P_L (MW)	Q_L (MVAr)	P_g (MW)	Q_g (MVAr)
1	1	1	0	0	0	0	0
2	0	1	0	0	0	0	0
3	0	1	0	3.151	0.631	0	0
4	0	1	0	1.2	0.24	0	0
5	0	1	0	0.92	0.185	0	0
6	0	1	0	0	0	0	0
7	0	1	0	0	0	0	0
8	0	1	0	0	0	0	0

A.3: Synchronous machine Data

Table A.3: Synchronous Machine data [15]

H (sec)	Xd (pu)	X'd (pu)	Xq (pu)	X'q (pu)	T'do(sec)	T'qo(sec)	Di
23.64	0.146	0.0608	0.0969	0.0969	8.96	0.31	0.0254

Table A.4: Synchronous Machine Exciter data [15]

KA	TA (sec)	KE	TE (sec)	KF	TF (sec)
20	0.2	1	0.314	0.063	0.35

A.3: DFIG Data

Table A.5: DFIG data [10]

H_t	H_g	R_s (pu)	X_s (pu)	R_r (pu)	X_r (pu)	X_m (pu)	K_{opt}
3.5	0.35	0.00488	0.09241	0.00549	0.09955	3.9528	0.56
K_{P2}	K_{I2}	K_{P3}	K_{I3}	ω_{base} (rad/s)	ω_s (pu)	S_{base} (MW)	V_{base} (V)
2.1	0.007142	0.034208	5.453926	314.16	1	2	690

APPENDIX-B
PARTICAL SWARM OPTIMISATION

Particle swarm optimization (PSO) is an evolutionary computation technique developed by Kennedy and Eberhart in 1995 [16]. PSO simulates the behaviors of bird flocking. In PSO, each single solution is a "bird" in the search space. It is called a "particle". All of particles have fitness values which are evaluated by the fitness function to be optimized, and have velocities which direct the flying of the particles. The particles fly through the problem space by following the current optimum particles.

PSO is initialized with a group of random particles (solutions) and then searches for optima by updating generations. In every iteration, each particle is updated by following two "best" values. The first one is the best solution (fitness) it has achieved so far (The fitness value is also stored.). This value is called pbest. Another "best" value that is tracked by the particle swarm optimizer is the best value, obtained so far by any particle in the population. This best value is a global best and called gbest. When a particle takes part of the population as its topological neighbors, the best value is a local best and is called lbest.

After finding the two best values, the particle updates its velocity and positions with following equation (A.1) and (A.2).

$$v[] = v[] + c1 * rand() * (pbest[] - present[]) + c2 * rand() * (gbest[] - present[]) \quad (B.1)$$

$$present[] = persent[] + v[] \quad (B.2)$$

v[] is the particle velocity, persent[] is the current particle (solution). pbest[] and gbest[] are defined as stated earlier. rand () is a random number between (0,1). c1, c2 are learning factors, usually c1 = c2 = 2.

The pseudo code of the procedure is as follows [17]:

For each particle
  Initialize particle
END
Do
  For each particle
    Calculate fitness value
    If the fitness value is better than the best fitness value (pbest) in history
      Set current value as the new pbest
  End
  Choose the particle with the best fitness value of all the particles as the gbest
  For each particle
    Calculate particle velocity according equation (B.1)
    Update particle position according equation (B.2)
  End
While maximum iterations or minimum error criteria is not attained

REFERENCES

[1] (Indian Wind Energy Association). *World wind energy installations grow, India slows down* [online]. Available: http://www.inwea.org/indiaslowsdown .htm

[2] (World Wind Energy Association) (2007, January, Monday 29). *WWEA expects 160 GW to be installed by 2010* [online]. Available: http://www.wwindea.org

[3] (MetaEfficient) Justin Thomas (2008, February, 3rd). *New Record: World's Largest Wind Turbine (7+ Megawatts)* [online]. Available: http://www. metaefficient.com/news/new-record-worlds-largest-wind-turbine-7-megawatts.html

[4] Chee-Mun Ong, *Dynamic Simulation Of Electric Machinery Using Matlab/ Simulink*, Prentice Hall, New Jersey, 001-626,1998

[5] G. D. Rai, *Non-Conventional Energy sources*, Khanna Publications, 1998.

[6] J. G. Slootweg, H. Polinder, and W. L. Kling, "Dynamic modelling of a wind turbine with doubly fed induction generator," in *Proc. IEEE Power Engineering Soc. Summer Meeting*, Jul. 2001, Vol. 1, pp. 644–649.

[7] Istvan Erlich, Jörg Kretschmann, Jens Fortmann, Stephan Mueller-Engelhardt, and Holger Wrede, "Modeling of Wind Turbines Based on Doubly-Fed Induction Generators for Power System Stability Studies," *IEEE Transactions on Power Systems*, Aug. 2007, Vol. 22, No. 3, pp. 909-919.

[8] Janaka B. Ekanayak, Lee Holdsworth, XueGuang Wu, and Nicholas Jenkins, "Dynamic Modeling of Doubly Fed Induction Generator Wind Turbines," *IEEE Transactions On Power Systems*, May 2003, Vol. 18, No. 2, pp. 803-809.

[9] L. Holdsworth, X.G. Wu, J.B. Ekanayake and N. Jenkins, "Direct solution method for induction wind turbines in models initialising doubly-fed power system dynamic" in *IEE Proc. on Generation, Transmission and Distribution.* May 2003, Vol. 150, No. 3, pp. 334-342.

[10] L. Holdsworth, X.G. Wu, J.B. Ekanayake and N. Jenkins, "Comparison of fixed speed and doubly-fed induction wind turbines during power system disturbances," in *IEE Proc. on Generation, Transmission and Distribution.* May 2003, Vol. 150, No. 3, pp. 343-352.

[11] J.B. Ekanayake, L. Holdsworth and N. Jenkins, "Comparison of 5th order and 3rd order machine models for doubly fed induction generator (DFIG) wind turbines," *Elsevier, Electrical Power Systems Research, 67*, 2003, pp. 207- 215.

[12] F. Michael Hughes, Olimpo Anaya-Lara, Nicholas Jenkins and Goran Strbac, "A Power System Stabilizer for DFIG-Based Wind Generation," *IEEE Transactions on Power Systems*, May 2006, Vol. 21, No. 2, pp. 763-772.

[13] Francoise Mei and Bikash Pal, "Modal Analysis of Grid-Connected Doubly Fed Induction Generators," *IEEE Transactions on Energy Conversion*, September 2007, Vol. 22, No. 3, 728-736.

[14] Pablo Ledesma and Julio Usaola, "Doubly Fed Induction Generator Model for Transient Stability Analysis," *IEEE Transactions on Energy Conversion*, June 2005, Vol. 20, No. 2, pp. 388-397.

[15] Peter W. Sauer and M. A. Pai, *Power System Dynamics and Stability*, Pearson Education, 2005.

[16] Eberhart, R. C. and Shi, Y., "Particle Swarm Optimization: Developments, Applications and Resources," *IEEE Congress on Evolutionary Computation 2001,* May 2001, 27-30 May 2001, Vol. 1, pp. 81-86.

[17] Xiaohui Hui, Yuhui Shi and Eberhart, R., "Recent advances in particle swarm," *IEEE Congress on Evolutionary Computation 2004*, June 2004, Vol.1, pp. 90- 97 .